Fast Response Estimation of Passively Controlled Structures Using Artificial Intelligence

Ausamah Al Houri

Submitted to the
Institute of Graduate Studies and Research
in partial fulfillment of the requirements for the degree of

Master of Science
in
Civil Engineering

Eastern Mediterranean University
September 2020
Gazimağusa, North Cyprus

Approval of the Institute of Graduate Studies and Research

<div style="text-align:right">

Prof. Dr. Ali Hakan Ulusoy
Director
</div>

I certify that this thesis satisfies all the requirements as a thesis for the degree of Master of Science in Civil Engineering.

<div style="text-align:right">

Prof. Dr. Umut Türker
Chair, Department of Civil Engineering
</div>

We certify that we have read this thesis and that in our opinion it is fully adequate in scope and quality as a thesis for the degree of Master of Science in Civil Engineering.

<div style="text-align:right">

Asst. Prof. Dr. Umut Yildirim
Supervisor
</div>

Examining Committee

1. Assoc. Prof. Dr. Mahmood Hosseini

2. Assoc. Prof. Dr. Rifat Reşatoğlu

3. Asst. Prof. Dr. Umut Yildirim

ABSTRACT

The research on the applicability of using passive control systems as a seismic mitigation approach and energy dissipating devices has grown significantly in the past decades with the focus on investigating the seismic response of the structure equipped with viscous dampers. In general, viscous damper as a device can be utilized for retrofitting and rehabilitating of old buildings, in addition, to optimize the cost of the new ones. When used in a structure, these structural dissipating devices can enhance the energy absorption capacity of the building under shaking intensities resulting in decreased displacements and acceleration responses. Current analysis approaches for finding a safe and optimized design is considered to be time and effort consuming since it requires several trial and errors to achieve the targeted responses. Nowadays, the literature is full with many high reliable estimation methods, such as artificial neural networks, that can be used to define a mathematical prediction model based on certain input parameters to reduce the need for doing a long trial and errors.

Therefore, the main objective of this study is to get benefit from these available estimation methods to propose a prediction models using ANN to obtain the response of structures equipped with viscous dampers from the behavior of the bare building. As a part of the study, thousands of numerical analyses by means of nonlinear response history analysis (direct integration method) are performed in order to estimate the response of various designs of bare and controlled reinforced concrete (RC) structures under different real earthquake records. Thereafter, the outputs of the numerical analyses will be used as an input for defining the coefficients of the estimation models using artificial neural networks (Levenberg-Marquardt backpropagation method) that

will be proposed in this study. The proposed estimation models require one-fourth of the time to build the model and determine the results in comparison to NTHA which results in faster, minimized cost and effort approach. In addition to that, the proposed prediction models exhibited high performance and accurateness in estimating the responses of RC structures.

Keywords: Reinforced concrete, optimization of dampers, damping, energy dissipation, artificial intelligence, estimation models, nonlinear response history analysis.

ÖZ

Pasif kontrol sistemlerinin bir sismik yük azaltma yaklaşımı ve enerji sönümleme cihazları olarak kullanılmasının uygulanabilirliği üzerine yapılan araştırmalar, viskoz damperlerle donatılmış yapının sismik tepkisinin araştırılmasına odaklanılarak son yıllarda önemli ölçüde artmıştır. Genel olarak, bir cihaz olarak viskoz damper, yeni uygulamaların maliyetini optimize etmek için ek olarak eski binaların güçlendirilmesi ve rehabilitasyonu için kullanılabilir. Bir yapıda kullanıldığında, bu elemanlar, sarsıntı yoğunlukları altında binanın enerji sönümleme kapasitesini artırabilir ve bu da yer değiştirmelerin ve hızlanma tepkilerinin azalmasına neden olur. Güvenli ve optimize edilmiş bir tasarım bulmak için mevcut analiz yaklaşımları, hedeflenen yanıtlara ulaşmak için birçok deneme ve hata içerdiğinden, zaman ve çaba gerektiren olarak kabul edilir. Günümüzde literatür, uzun bir deneme ve hata oranını azaltmak için belirli girdi parametrelerine dayalı bir matematiksel tahmin modelini tanımlamak için kullanılabilen yapay sinir ağları gibi birçok yüksek güvenilirlikli tahmin yöntemiyle doludur.

Bu nedenle, bu çalışmanın temel amacı, sade (kontrolsüz) binanın davranışından, viskoz sönümleyicilerle donatılmış yapıların tepkisini elde etmek için yapay sinir ağını kullanan bir tahmin modelleri önermek için bu mevcut tahmin yöntemlerinden yararlanmaktır. Çalışmanın bir parçası olarak, sade (kontrolsüz) ve kontrollü betonarme yapıların çeşitli tasarımlarının farklı gerçek deprem kayıtları altındaki tepkisini tahmin etmek için doğrusal olmayan davranış geçmişi analizi (doğrudan integrasyon yöntemi) aracılığıyla binlerce sayısal analiz yapılacaktır. Bundan sonra

sayısal analizlerin çıktıları, bu çalışmada önerilecek tahmin modellerinin katsayılarının tanımlanmasında girdi olarak kullanılacaktır.

Anahtar Kelimeler: Betonarme, sönümleyicilerin optimizasyonu, sönümleme, enerji sönümleme, yapay zeka, tahmin modelleri, doğrusal olmayan tepki geçmişi analizi.

DEDICATION

I would like to dedicate this to my family, friends and everybody who believed in me. I would to like express my gratitude towards my mom, dad and my brothers. In addition, I would like to thank from deepest of my heart my uncle and his wife for their huge support since without them I would not be able to be here and achieve this.

ACKNOWLEDGMENT

I would like to express my gratitude to my supervisor Assist. Prof. Dr. UMUT YILDIRIM for his continuous help and support, where without his motivations this study would have never taken shape.

In addition, I would like to gratefully thank the academic staff of the civil engineering department for their help during my master degree study.

Furthermore, I would like to acknowledge and thank my friend and colleagues.

Finally, it is important to thank my family who without their care, support, and motivation I would have never get to this point.

TABLE OF CONTENTS

LIST OF TABLES

LIST OF FIGURES

LIST OF ABBREVIATIONS

ANN   Artificial Neural Network

C   Damping Coefficient

FVD   Fluid Viscous Damper

MSE   Mean Square Error

NTHA   Nonlinear Time History Analysis

PEER   Pacific Earthquake Engineering Research Center

PGA   Peak Ground Acceleration

PGD   Peak Ground Displacement

PGV   Peak Ground Velocity

R^2 Coefficient of Determination

RC   Reinforced Concrete

RMSE   Root Mean Square Error

RSN   Record Sequence Number

trainlm   Levenberg-Marquardt backpropagation

α   Velocity Exponent

Chapter 1

INTRODUCTION

1.1 General Introduction

During earthquakes which is considered one of the most catastrophic and disastrous natural phenomena, all types of structures and infrastructures including buildings, bridges, airports, etc… will shake due to the stochastic shaking intensity resulting in drastic damage to structural and non-structural elements. This can be attributed to the energy dissipation mechanism and the factors taking role including rebar slip, rebar yielding, cracking, and spalling of concrete [1]. Therefore, the research has grown rapidly over the past decades with the aim on investigating techniques for retrofitting and rehabilitating the RC structures by means of increasing the load-carrying capacity by adding external confinement and shear reinforcement [2], introducing new structural elements to the structure such as shear walls or equip the structure with the energy dissipating devices such as dampers to increase the absorbed energy during earthquakes. The utilization of dampers in the structure has shown to be very effective in decreasing the effects of the earthquake on the crucial components of the structure by absorbing the seismic energy leading to a reduction in structural response (displacement and acceleration). However, it is still difficult, time and effort-consuming to identify the optimization methodology for the dampers in the structure since it depends on an iterative process of analyzing and redesigning using accurate but challenging analysis techniques such as time history analysis which is the most accurate analysis for assessment of structures but it has some issues that limits or

complicates the usage of this technique including the limited capability of the available commercial software in handling this type of analysis, the difficulty to perform and interpret the results of time history analysis due to the complexity in selecting the suitable ground motion inputs and the time and effort consuming this procedure takes due to the fact that the design passes through a trial and error process to optimize the size of the passively dissipating devices that can meet the requirements of the standards in terms of maximum allowable drift ratio.

1.2 Aim of the Study

The aim of the study is to propose and suggest a mathematical estimation model using artificial intelligence capable of obtaining the response of structure utilized with the damper device. Therefore, numerical study will be performed in order to obtain the response in the time domain and as peak (envelope) of different types of structures using nonlinear time history analysis that will be performed on different types of structures equipped with passive controllers under different characteristics of ground motion inputs in order to identify the important factors needed to be taken into consideration for establishing the mathematical estimation models. However, the estimation model will be developed based on multiple simple cases of fluid viscous damper (FVDs) configuration in the structure where dampers are positioned as a zig-zag shape in the mid-bay and thus, other configurations of FVDs were not taken into account during the formation of input dataset because the aim of the thesis is to investigate the applicability of estimating the responses in the time domain and as peak (envelope) of RC structures equipped with FVDs using ANN. On the other hand, the prediction model is intended to be applied to estimate the responses of RC low, low-to-mid-, and mid-rise structures to cover the wide range of common buildings in the Middle East. This can be achieved by evaluating and specifying the critical factors

impacting the response of the structure through an excessive number of nonlinear time history analysis on wide and different types of structures under different characteristics of ground motion records. Then, establishing an estimation model via artificial intelligence using the results obtained from the nonlinear time history analysis to estimate the responses of RC structures equipped with FVDs.

Chapter 2

LITERATURE REVIEW

2.1 Introduction

This section presents a review of the literature which focuses on the passive control systems specifically FVDs and their optimum parameters in RC structures were considered and highlighted. Despite the fact that many papers had discussed and established novel estimation models for uses in structural engineering, very limited studies used these models in passive control systems. Accordingly, the main aim of this study which is to establish a mathematical estimation model capable of predicting the seismic response of RC structure equipped with viscous damper based on RC bare structure using ANN under wide range and different characteristics of ground motion records is considered to be an original and new application of such mathematical estimation models in the structural area. Therefore, within the frame of this section useful information from the literature related to both FVDs and ANNs is going to be obtained and discussed.

2.2 Seismic Control of Structures Using FVDs: Recent Advances in the Literature

Structural vibration is commonly existed phenomenon in several fields of engineering including machinery, aerospace, and civil engineering [3], such actions arise significant issues related to the safety of structure by the imposed demand on the machine or building components. Nowadays, several control strategies including passive systems such as dampers (FVDs, steel friction dampers, and viscous elastic

dampers) and base isolators, and semi-active systems and full active control ones are being adapted all over the world to provide a way of reducing these actions and ensure a safe behavior of the structural system. In fact, FVDs are well-established devices that can provide a supplemental passive energy dissipation capability to structures in earthquake-prone countries for seismic mitigation and protection [4]. By means of design, FVDs are considered as a velocity-based dissipative system that is capable of generating viscous damping in the case of the internal fluid going in the special orifices. These devices were first introduced to the world in 1862 when the British army used them in cannon launchers to decrease their movement when firing cannonballs [5]. At their early age, FVDs were mainly used as military equipment and supplemental to industrial machinery [6, 7]. However, the recent intentions over the last few decades in the construction industry represented by finding novel solutions and strategies for seismic protection and mitigation, in addition to the overwhelming advances in the structural analysis approaches, these devices found its way to structural engineering and currently are being utilized in many countries all over the world [8, 9, 10, 11, 12].

2.2.1 Structure Response Analysis Subjected to Earthquake and Implemented with Nonlinear FVDs

The process of performing modal analysis in order to calculate the vibration response of the main structure can be quite challenging due to the nonlinear damping behavior of the nonlinear FVDs even if the assumption that the damping in the superstructure is proportional was made because the damping of the building plus damper is not proportional [13, 14]. Similarly, making the assumption that the main structure is linearly behaving while the structure plus damper system has inherent nonlinear characteristics can lead to a failure in the response spectrum technique and hence

complicate the design of the damper and/or the evaluation of the structure response [15]. Therefore, an effective approach for calculating the vibration response known as the equivalent viscous damping ratio gained acceptance and popularity among scholars. However, this ratio is determined by assuming that the dissipation energy of equivalent linear viscous damping is equal to the dissipation energy of an equivalent nonlinear viscous damping during one vibration cycle which is used by [16, 17] as an effective approach for overcoming the complexities during designing nonlinear viscous dampers but only under the assumption of harmonic motion [18, 19]. Nonetheless, this assumption is not always valid since the motion of a natural earthquake is not harmonic but rather random that possesses nonstationary characteristics and thus, the equal dissipation energy method is not capable of accurately estimating the real effects of a nonlinear viscous damper on the response of the structure [15]. To surpass this issue, power spectral density function that is consistent with the elastic response spectrum of various building codes was suggested by [20] by means of using stochastic analysis and statistical linearization approach [21, 22, 23, 24] to determine the equivalent damping ratio of single and multi-degree of freedom. Another solution for linear and elastic properties of the main structure to solve this difficulty is the establishment of real value modal response history analysis of elastic two-way asymmetric structure [13]. However, the nonlinear and inelastic properties of the main structure, a solution based on a simplified numerical algorithm that combines force analogy and state-spaced methodologies for NRHA of structures utilized with nonlinear FVDs was suggested by [25]. Furthermore, a simplified direct evaluation approach that is consisted of linearization of the nonlinear viscous damper and linearization of nonlinear structure was used for estimating the seismic response of nonlinear structure incorporated with nonlinear viscous damper [26]. Another

method for estimating the seismic performance of structure equipped with nonlinear viscous damper based on probabilistic approaches was conducted by [27]. This method was derived from probabilistic approaches based on the fact that earthquakes inherent nonstationary properties and hence, a nonstationary stochastic response can be used to investigate the seismic response of structures [28]. Therefore, performing response analysis of structure utilized with nonlinear FVDs subjected to ground motion effects is inevitable and necessary for studying the different design methods and/or the seismic behavior of the nonlinear viscous damper.

2.2.2 Design of the FVD

The design of nonlinear FVD is highly influenced by many properties including the damping coefficient C, velocity exponent α, and the placement of the damper [14]. Therefore, adopting adequate design parameters results in a better damping performance. As the degree of nonlinearity of FVD is dependent on the value of α, it affects the seismic behavior of the structure dramatically [29]. Furthermore, the placement of the damper plays a crucial role throughout the designing procedure [30]. Thus, different performance indices were applied in order to define the optimum values of C and α such as the force index and performance index which was developed by [31]. While the force index is related to the nonlinear properties of FVD by means of minimizing the damping force in the damper, the performance index is associated with the structure response including peak inter-story drifts angle and peak floor accelerations. However, and due to the difficulty in designing nonlinear FVD, the equivalent linearization method was suggested as one of the effective solutions for such types of complex designs. The concept of the equivalent linearization method proposes the construction of a nonlinear system for a certain criterion then transform it to an equivalent linearized system [32]. Therefore, this method can be applied by

assuming that the energy dissipation of nonlinear FVD is equal to linear FVD using energy or power consumption approach. The energy consumption approach states that the equivalent viscous damping of nonlinear FVD is the same as the equivalent linear viscous damper in one vibration cycle and thus an equivalent linear system could be constructed [33]. Moreover, an empirical relationship was established between the spectral pseudo-velocity and the actual relative structural velocity where the actual velocity of the nonlinear viscous damper was determined and using the concept of energy consumption method, the actual velocity of the nonlinear viscous damper is used in order to derive the equivalent viscous damping of the nonlinear viscous damper [34].

2.2.3 Theoretical Definition

The two categories of the viscous damper in terms of producing damping force are viscous damping wall [35, 36, 37] and rod type viscous damper [38, 39]. The main parts of the viscous damping wall are viscous fluid, upper floor, two lower floors, one inner and two outer plates. The inner plate is attached to the upper floor whereas the two outer plates are connected to the two lower floors. Regarding rod type viscous damper, the main parts are the cylinder, fluid with high velocities such as silicon oil, piston head, piston rod, chambers, seal, seal retainer, and orifices. The vibration energy in the viscous damping wall that is subjected to wind or earthquake excitation is dissipated by means of internal friction initiated in the viscous material. This friction is generated due to the relative motion of the inner plate with respect to the outer plate resulting in alternating shear movement of the inner plate inside the viscous fluid. With regard to the rod type viscous damper under wind or earthquake excitation, the vibration energy is dissipated by means of pressure difference as the fluid flows between the two ends of the chambers through orifices due to the relative movement

of the piston with respect to the cylinder. However, the following equation describes the relationship of the damping force and velocity which was adopted by [18] based on the simplified Maxwell model:

$$F_d = Csgn(\dot{u})|\dot{u}|^\alpha \qquad (2.1)$$

The C is the coefficient of damping while α is the velocity exponent and sgn (.) is the signum function. α represents the degree of nonlinearity of the viscous damper and ranges between 0.1 to 2. $\alpha < 1$ represents nonlinear viscous damper, $\alpha = 1$ represents linear damper and $\alpha > 1$ represents ultra-linear viscous damper. Viscous damper with $0.1 < \alpha < 0.5$ is used as earthquake-resistant device [15] while for $0.5 < \alpha < 1$, the viscous damper is used to resist to combined effects of both wind and earthquake loads [7]. Under near fault earthquakes, structures with a long period that is utilized with linear viscous damper generates a very high amount of damping force due to the proportionality of damping force and relative velocity [19] resulting in potential inefficiency in the damper developed by deficient and poor strength at the connectors leading to inability to dissipate no more vibration. However, both linear and nonlinear viscous damper can produce the same damping effect but nonlinear viscous damper shows better results in terms of decreasing the damping force in contrast to linear viscous damper [14]. As a result, the nonlinear viscous damper is superior to linear viscous damper by means of economical and structural aspects [40, 41, 31]. In addition to that, nonlinear viscous damper possesses higher energy-dissipating capacity due to its hysteretic loop shape that can be described to be a plumber than a linear viscous damper whose hysteretic loop is quite similar to an ellipse [33] as illustrated in Figure 1.
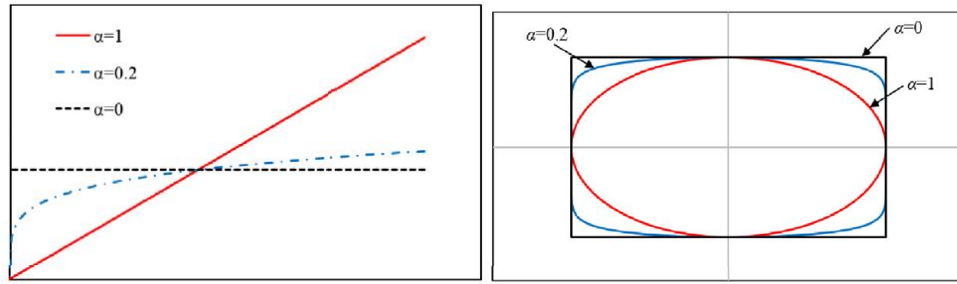
Figure 1: Behavior FVD at several α for force velocity relation and force displacement relation [13]

Moreover, under shocking, ground motions, winds loading cases, the nonlinear viscous damper can exhibit adequate and suitable damping behavior [18] along with tolerating and overcoming the effect of higher modes on the response of the structure [42, 43].

2.2.4 Applications of FVDs in Civil Engineering Field

In the beginning, the use of FVDs was mainly for military purposes to reduce the movement of the cannons while firing cannonballs. However, as FVDs proved its effectiveness in military applications, the interest started to increase in adopting them for commercial purposes specifically in building and bridge applications to meet the optimal performance of these structures under the effect of seismic, wind or other vibrating disturbance sources. The significance of using these devices arises from the fact they are capable of dissipating very large amount of the energy produced by strong-motion including earthquake or wind or etc. at relatively low cost without comprising the structure to any localized damage which can result in collapse or failure in case of not using FVDs. However, in order to achieve the best performance of FVDs, consideration must be made to assure that the damper forces do not add to the overall stress of the structure but it should decrease the stress and deflection in the structure simultaneously by the adequate placement of the dampers. The use of FVDs to resist the wind excitation started in 1993 and for seismic in 1995. Nowadays, there

are more than 80 large structures around the world equipped with FVDs to resist seismic or wind loads including the Arrowhead regional medical center in California and the pacific northwest baseball stadium in Washington [44].

2.3 Artificial Neural Networks

ANNs are very similar to those biological neurons in the brain and hence the name is inspired by them. They can be described as the mathematical functions of the tree of neurons linked to each other or simply as the processing elements of the collective networks of artificial neurons as defined by [45] which can be sorted into input, hidden, and output layers. The input layer governs the input data and inconstant factors whereas the hidden layer contains the computational procedure done via the neurons and the output layer which consists of the solution being considered as shown in Figure 2.
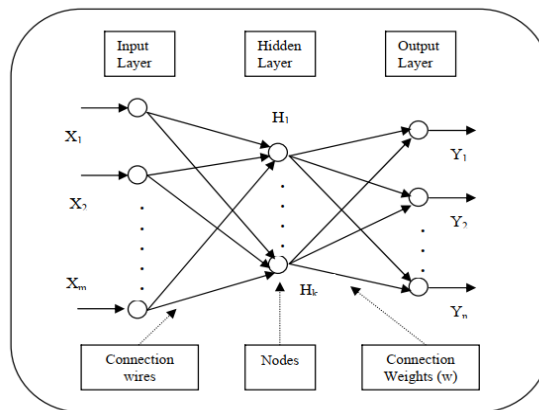

Figure 2: ANN modelling system

This process of obtaining input data, computing, and extracting the result as output is done by each neuron as stated by [46]. However, these neural networks must be trained in order to achieve the best set of parameters for obtaining the highest accuracy of neural networks by minimizing the errors accompanying the output using a learning

algorithm. ANN is described as the learning process by imitating the biological parent brain via collecting knowledge by identifying the patterns of the data and learn accumulatively through experience [47]. This learning process needs to be tested and if it is valid and adequate, ANN will be able to produce generalized fundamentals to estimate the needed output data limited by the domain used in the training examples. This characteristic of ANNs is highly important and useful for engineers including civil engineers since it is capable of learning from the training examples and produce generalized solutions [48]. On the other hand, there are different types of neural networks includes single-layer feedforward, lattice structures, recurrent networks, and multilayer feedforward which is considered the most prevailing type of network. Nonetheless, ANNs exhibited better estimation of cost in comparison to classical approaches due to the ability to train it and its capability to learn and produce reliable results [46]. ANN is a technique adopted to learn, produce, and constitute knowledge [49].

2.3.1 Methods of Training

Backpropagation learning methods

It can be described as neurons incorporated and stored in multiple layers within a network. These multiple layers are the input layer which includes the input data and variable parameters whilst the hidden layer holds the data processing through the iterative procedure and the output layer is the layer where the results of a specific problem are attained. Despite the fact that backpropagation is considered to be the most popular and predominant approach of learning because of its capacity to identify the data patterns using nonlinearity principles, one of its shortcomings is what known as the step size problem which arises from the necessity to set a small yet random number for each parameter (weight) so that each neuron will adjust to a different set

of weights resulting in a very slow process where the solution is determined via decreasing the slope and thus the overall error of every parameter to a minimum value. However, if the step size is too big, the network may exceed the global minimum leading to overfitting while if the step size is too small, the network may get to the local minimum leading to underfitting. Another drawback is the moving target problem which occurs when the parameters in each neuron adapt separately to detect a unique feature while the other weights are changing constantly resulting in fluctuation in these weights as they evolving leading to the term herd effect where some neurons detect a specific feature and eliminate others till the error of that feature is dismissed then moving to the other features and ignore that feature resulting in a loop or dance between these features where it may take a long time before these features are defined at the same time. However, the neural network showed superior results in terms of the performance in contrast to the linear regression model as concluded by [45] when fixing training data and parameters for both models.

BFGS Quasi-Newton Backpropagation

This type of algorithm is quite useful for a small scale of weights as it requires extensive computation process and storage [50]. In addition to that, this method is applicable to nonlinear optimization problems via trial and error procedures [51] . The solution can be obtained when the slope approaches zero or the value set precedently [52] and the training function is given in equation 2.2.

$$x_{k+1} = x_k - A_k^{-1}\nabla f(x_k) \qquad (2.2)$$

Bayesian Regularization Backpropagation

The effectiveness of this approach arises from the fact that it can reduce or erase the cross-validation by converting the nonlinear regression to an arranged statistical

13

problem represented via ridge regressions [53]. However, and unlike other training methods, this method is based on the probability distribution of artificial network weights rather than reducing the function error to obtain the optimal weights set [54, 55]. Moreover, this approach is favorable due to the low probability of reaching overfitting because it excludes the validation necessity ending with the result withing the required criteria, the capability of creating a representative mathematical model for all the data. The training function of this approach is illustrated in equation 2.3.

$$S(w) = \sum_{i=1}^{N_D} [y_i - f(X_i)]^2 + \lambda \sum_{i=1}^{N_P} w_j^2 \qquad (2.3)$$

Conjugate Gradient Backpropagation with Powell-Beale Restarts

Unlike BFGS Quasi-Newton Backpropagation method, this approach needs no storage and acquires a small number of functions to characterize the parameters making the solution converges to linear state. However, this approach relies upon the pattern of the data at the slope as described in equation 2.4 [56].

$$|\nabla_{k-1}^T \nabla_k| \geq \alpha \|\nabla_k\|^2 \qquad (2.4)$$

Conjugate gradient backpropagation with Fletcher-Reeves updates

It consists of setting the sharpest vertical slope on the declining axis then adjusting it using equation 2.5 then applying equation 2.6 [57].

$$B_k = \frac{\nabla_k^T \nabla_k}{\nabla_{k-1}^T \nabla_{k-1}} \qquad (2.5)$$

$$P_k = -\nabla_k + B_k P_{k-1} \qquad (2.6)$$

Levenberg-Marquardt backpropagation

It is based on Gauss-Newton and gradient descent methods which were mainly originated to solve nonlinear least-square functions [58, 59, 60] using the adaptive pattern [61]. However, this method is insufficient to produce the optimum results in case of describing gradient descent as the backpropagation [62] whereas if

14

backpropagation is described as Gauss-Newton, it can show the best and optimum results [63]. The training approach is illustrated in equation 2.7 [64].

$$\Delta X_k = -[J^T(x_k)J(x_k) + \mu_k I]^{-1}J^T(x_k)v(x_k) \qquad (2.7)$$

Chapter 3

RESEARCH METHODOLOGY

3.1 Introduction

This section will be devoted to discussing the adopted research strategy in this study. In the beginning, the basis for the parametric study will be presented by highlighting the need and influence of each parameter. In addition to that, the preliminary analysis and the nonlinear modeling of RC 2D bare structures using nonlinear response history will be described together with the properties of FVDs. The second section will focus on the methodology behind the selection of the appropriate training method for ANN. Furthermore, the approach for establishing the mathematical estimation models generated via the ANN after performing an extensive number of time history analyses in order to produce accurate models capable of predicting the response of RC structures utilized with FVDs will be provided.

3.2 Basis of the Parametric Study

In order to make a good prediction model many data need to be used for training, testing, and validation of the neural networks and hence, 70% of the data will be used in training, 15% will be used in testing, and the last 15% in validating since this distribution showed the best results [65]. These data are the responses of the NTHA of 9 models that represent low, low-to-mid, mid, and high-rise buildings as illustrated in Table 1. Accordingly, the following parameters are suggested to conduct a parametric study that includes different models. This parameter represents the weight and stiffness of a building in a given direction. Based on this value, the seismic demand

is obtained from the response spectrum shape of the time history record. Therefore, to propose a model with a wide range of applications, nine different values of periods are proposed in this thesis to simulate the behavior of low, mid, and high-rise RC buildings. The periods in Table 1 are relatively bigger than the corresponding usual values for such models. This is attributed to the fact that in nonlinear analyses, it is very important and crucial to model the lateral stiffness of the structural elements using effective rigidity in order to investigate the performance of the structure under seismic conditions accurately and efficiently. Based on that, a reduction in the stiffness will occur leading to an increase in the periods of the models. Each case of these structures has different column dimensions, steel reinforcement ratios, and concrete grade while the beam section is left constant to limit the difference in the bare structure models to the lateral stiffness only. These structural models were divided into two groups where the first group (group Training) is for forming a database for training and the other group (group Validation) is for validating the prediction model.

Table 1: Selected bare structures for training and validating the prediction models

Model No.	First mode period (s)	Column dimensions (cm)	Steel reinforcement ratio (%)	Concrete grade	Usage
1	0.2054	30×30	1.37	C16	Training
2	0.29488	35×35	1.51	C16	Validating
3	0.38209	40×40	1.16	C16	Training
4	0.4685	45×45	1.59	C20	Validating
5	0.55914	50×50	1.76	C25	Validating
6	0.63287	60×60	2.18	C30	Training
7	0.73781	65×65	2.51	C30	Validating
8	0.84333	70×70	3.02	C35	Validating
9	0.94481	80×80	3.08	C35	Validating

3.3 Nonlinear Finite Element Modeling

NIST GCR 17-917-46v3 guidelines published by the National Institute of Standards and Technology [66] were followed for nonlinear modeling of the RC structures. The fiber section hinges were taken into account by generating the confined compressive stress-strain behavior as illustrated in Figure 3 using the unconfined stress-strain model and the reinforcement configuration of the structural section following and adopting an approach suggested by Mander et al. [67]. However, the stress-strain relation of steel reinforcement was followed and adopted from Park & Paulay model [68] as illustrated in Figure 4.
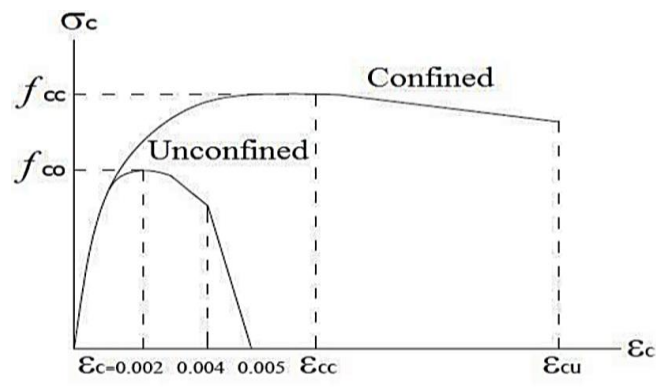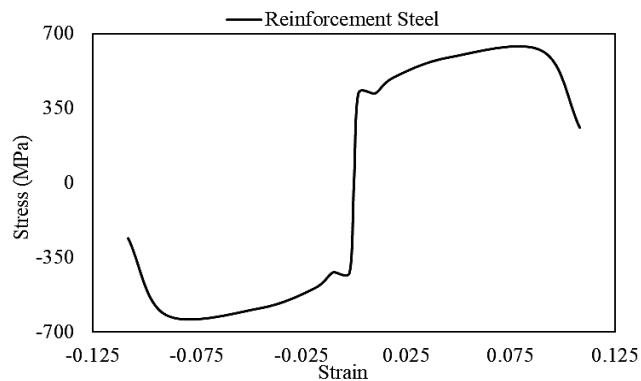

Figure 3: Concrete stress-strain behavior

Figure 4: Steel reinforcement stress-strain behavior

Under natural hazard such as earthquakes, RC members undergo to high change and may exceed its crack section [69]. Thus, in nonlinear analyses, it is very essential and significant to model the lateral stiffness of the structural elements using effective rigidity in order to assess the performance of the structure under seismic conditions accurately and effectively. As a result, and using the following equations (Eq 3.4 and 3.5) that are suggested by Kwon [70] to determine the effective rigidity in beams and columns

$$\alpha = 0.003DR^{-0.65} + \gamma \leq 0.8 \tag{3.4}$$

$$\gamma = (-50\rho_T + 2.5)\left(\frac{P}{A_g f_c'}\right)^{(-20\rho_T + 2.15)} + (15\rho_T + 0.05) \tag{3.5}$$

where;

α= Stiffness Reduction Factor in Beams and Columns.
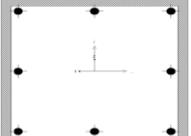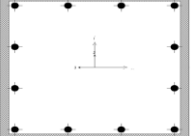
P= Axial Load.

A_g= Member Gross Sectional Area.
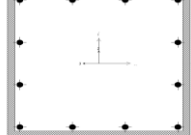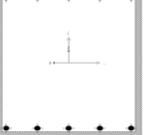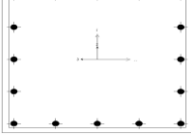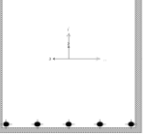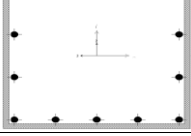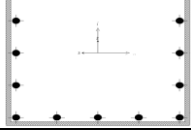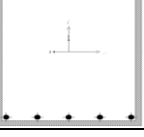
f_c'= Compressive Strength of Concrete.

ρ_T= Longitudinal Tension Reinforcement Ratio

DR= Story Drift Ratio Assumed to be 0.008 to Predict the Stiffness of Elements at First Yield (the most popular scenario in frame members under MCE_R ground motions) [66].

The concentrated hinge model was selected to simulate the nonlinear behavior of the structural members in agreement with Kalantari and Roohbakhsh [71] approach that requires subdividing the fiber parts inside the beams and columns sections into cover, core, and steel reinforcement fibers where cover is built with unconfined concrete model and core which is built with the confined concrete model. However, the

Rayleigh damping approach was followed to demonstrate the damping inherited in a normal concrete structure during the nonlinear direct integration analysis by means of computing α and β coefficients to provide a 2.5% damping ratio at 0.25 and 1.5 of the first fundamental mode period. Lastly, P-Δ effects were taken into account during the analysis while soil-structure interactions were neglected via assuring the stability of the structure by fixing the lower nodes in each column resulting in no rotation or displacement at the base of the frames. Additionally, beam to column panel zones was implemented without simulating the joint stiffness directly but rather through the use of line elements that is emerged from the beams and columns into the panel zone as stated in NIST GCR 17-917-46v3 [66].

Model No.	Column Section	Beam Section
1		
2		
3		
4		
5		
6		

7		
8		
9		
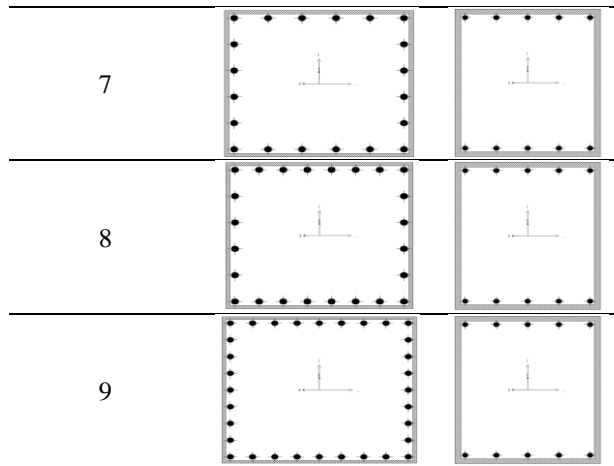
Figure 5: Column and beam sections of bare structure finite element models

Model No.	Selected System
1-2	
3-4	
5-6	

21

7-8

9
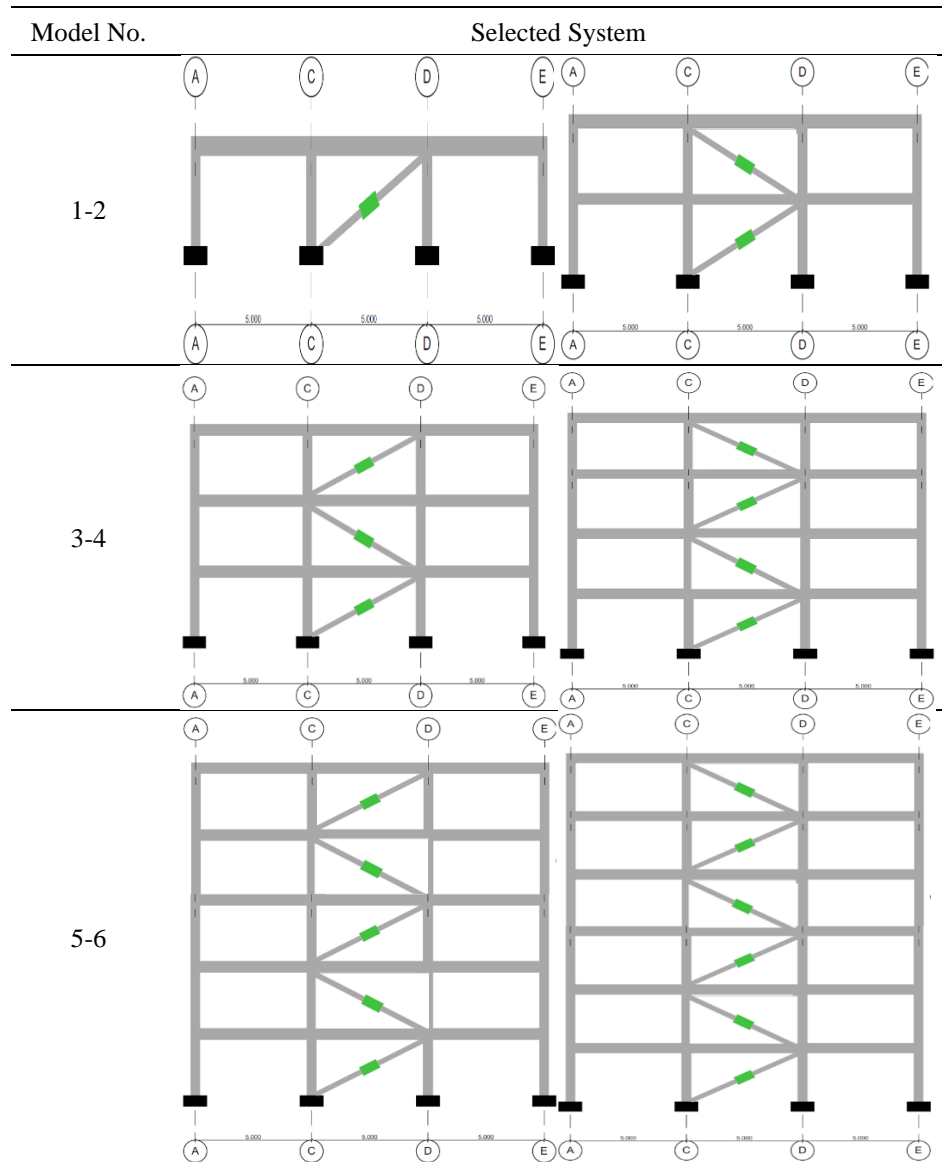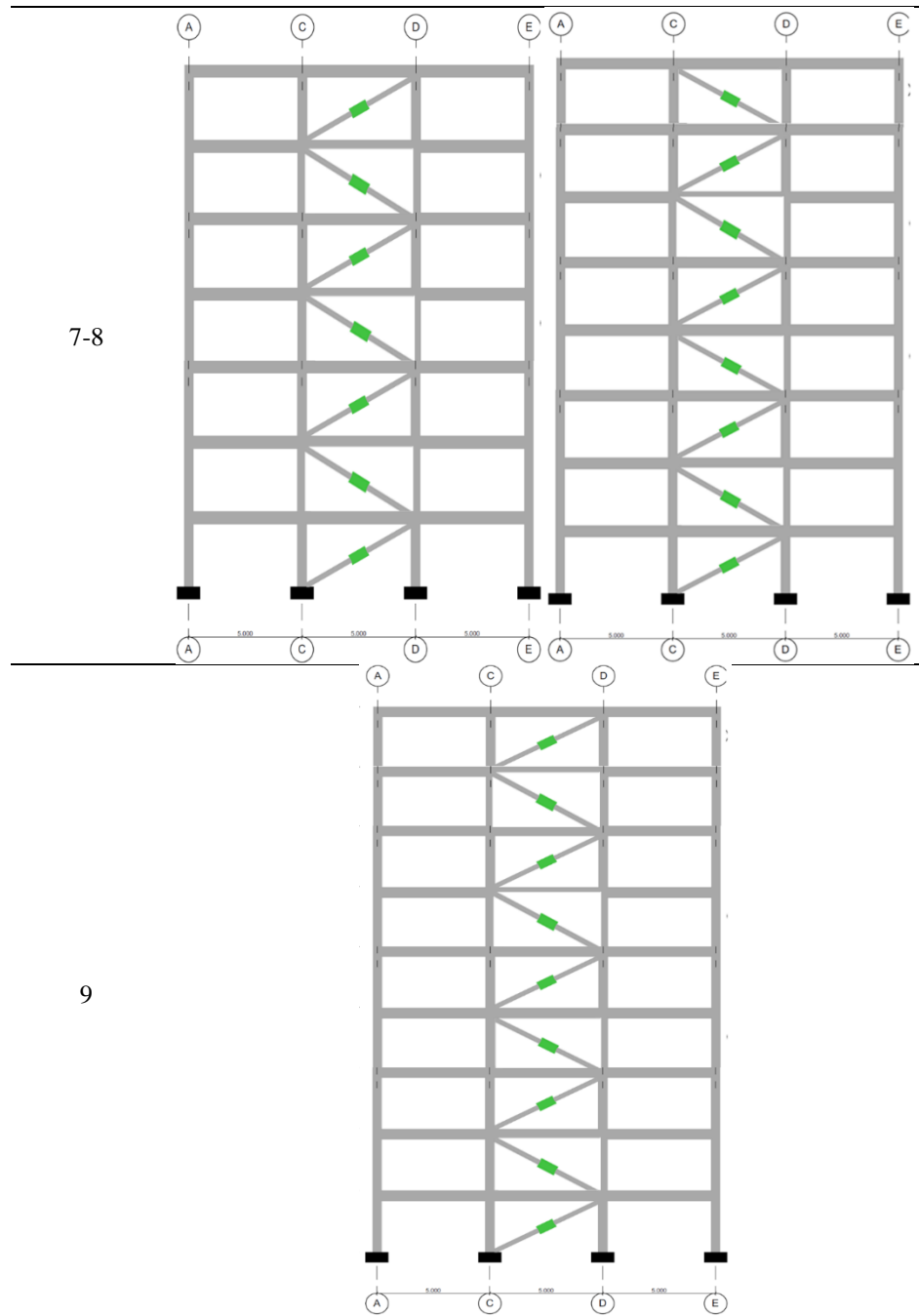
Figure 6: Selected 2D finite element model structures for establishing the estimation models

The estimation models will be developed based on multiple simple cases of FVDs configuration in the structure where dampers are positioned as a zig-zag shape in the mid-bay as illustrated in Figure 6 and thus, other configurations of FVDs were not taken into account during the formation of input dataset because the aim of the thesis

is to investigate the applicability of estimating the responses in the time domain and as peak (envelope) of RC structures equipped with FVDs using ANN.

3.4 Earthquake Records

The earthquake intensity is a very important parameter than needs to be considered as it changes the forces on a structure. Therefore, in this study, 18 different earthquake records were used to cover a wide range of ground motion types which can improve the prediction model and extend its capability for most of the earthquake types. The 18 natural selected ground motion records were downloaded and collected from the Pacific Earthquake Engineering Research Center (PEER) as three sets of 6 records. These sets were categorized into a near fault, far fault, and pulse-like. However, differentiating the pulse like records form non-pulse like can be very difficult and problematic. Therefore, equation 3.1 known as pulse indicator I_p was suggested by [72] to indicate pulse-like records. Moreover, the three requirements that needed to be met in order to specify the ground motion record as pulse-like are I_p greater than 0.85, PGV greater than 0.85, and the time $t_{20\%,orig}$ at 20% of the total cumulative squared velocity for original ground motion greater than the time $t_{10\%,pulse}$ at the 10% of the total cumulative squared velocity for the extracted pulse [73].

$$I_p = \frac{1}{1+e^{-23.3+14.6(PGV\ ratio)+20.5(energy\ ratio)}} \tag{3.1}$$

The following table illustrates the characteristics of ground motion records that were taken into consideration as the selection criteria which include peak ground acceleration, peak ground velocity, shear wave velocity of the soil profile, and etc.

Table 2: Selected Earthquakes

Group	RSN (Record Sequence Number)	Year	Earthquake Name	Tp (s)	Magnitude (Mw)	Vs30 (m/s)	Duration (s)	PGA (g)	PGV (m/s)
Near-Fault	126	1976	Gazli, USSR	-	6.8	259.59	14	0.702	0.662
	564	1986	Kalamata, Greece-01	-	6.2	382.21	30	0.239	0.335
	949	1994	Northridge-01	-	6.69	297.71	40	0.345	0.411
	1494	1999	Chi-Chi, Taiwan	-	7.62	460.69	90	0.146	0.460
	3943	2000	Tottori, Japan	-	6.61	616.55	300	0.274	0.153
	3979	2003	San Simeon, CA	-	6.52	362.42	81	0.179	0.128
Pulse-Like	159	1979	Imperial Valley-06	2.338	6.53	242.05	29	0.287	0.349
	802	1989	Loma Prieta	4.571	6.93	380.89	40	0.514	0.416
	828	1992	Cape Mendocino	2.996	7.01	422.17	36	0.591	0.493
	1182	1999	Chi-Chi, Taiwan	2.5704	7.62	438.19	150	0.359	0.423
	4040	2003	Bam, Iran	2.023	6.6	487.4	67	0.808	1.241
	6897	2010	Darfield, New Zealand	7.826	7	295.74	138	0.257	0.394
Far-Fault	17	1952	Southern Calif	-	6	493.5	40	0.036	0.031
	56	1971	San Fernando	-	6.61	235	40	0.071	0.047
	68	1971	San Fernando	-	6.61	316.46	80	0.225	0.217
	169	1979	Imperial Valley-06	-	6.53	242.05	100	0.236	0.263
	295	1980	Irpinia, Italy-02	-	6.2	476.62	32	0.018	0.031
	325	1983	Coalinga-01	-	6.36	522.74	65	0.0260	0.036

The scaling of ground motion records can be performed using numerous and wide range approaches including ATC-63 [74] approach, ASCE/SEI 7-05 [75] approach, and minimizing mean square error (MSE) approach [76]. Michaud and Léger [77] investigated a couple of scaling approaches including the ones mentioned previously and concluded that MSE scaling technique showed superior results in contrast to ACT

and ASCE approaches. Based on that, the MSE scaling approach was selected in this thesis to scale the 18 ground motion records for a range of periods from 0 to 5 seconds to match the targeted spectrum as illustrated in Figure 7. To scale the ground motion records using the MSE technique, the single scale factor f was determined for each record (Eq 3.2) then these calculated factors were adjusted using adjustment parameter to minimize the value of MSE (Eq 3.3) between the mean spectrum of the scaled records and the target spectrum in order to achieve the best match between the mean spectrum of final scaled ground motions and the target spectrum over the period range of interest [76]. Later, the addition of 15 successive zeroes at the end of each record was performed to include the free vibration response of the structure after excitation [78].

$$f = \frac{SA^{target}(T_s)}{SA^{record}(T_s)} \tag{3.2}$$

where;

f = Linear Scale Factor.

$SA^{target}(T_s)$ = Target Spectral Acceleration at Specific Period.

$SA^{record}(T_s)$ = Record Spectral Acceleration at Specific Period.

$$MSE = \frac{\sum_i w(T_i)\{ln[SA^{target}(T_i)] - ln[f * SA^{record}(T_i)]\}^2}{\sum_i w(T_i)} \tag{3.3}$$

where;

MSE = Minimizing Maximum Error.

$w(T_i)$ = Weight Function (usually equal 1).
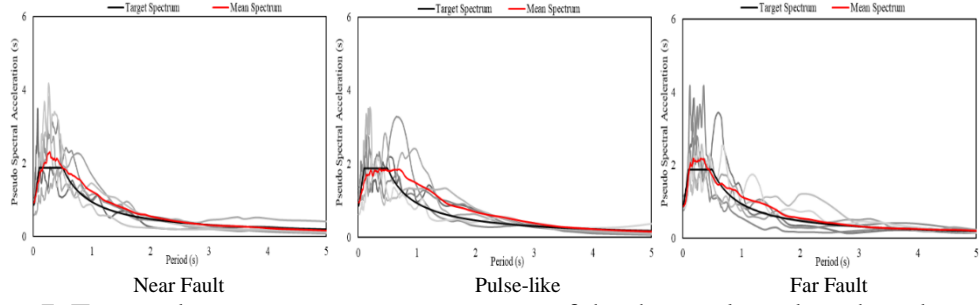
Figure 7: Targeted spectrum vs mean spectrum of the three selected earthquake groups

3.5 Parameters of the Fluid Viscous Dampers

As a matter of fact, FVDs are velocity-dependent systems that work by means of damping force which is intended to sustain the applied forces on the structural system without influencing the period of the structure, unlike base isolators. The damping force of FVDs is given by the following expressions as discussed in chapter 2.

$$F_d = Csgn(\dot{u})|\dot{u}|^\alpha \tag{3.4}$$

where C is the damping coefficient for the viscous damper, representing the energy-dissipation capacity independent of the α value which is related to the internal configuration of the viscous damper (e.g., orifices) and sgn (.) is the signum function. Based on this equation, the C and α are the constants that significantly changes the damping force. Accordingly, a combination of five different values of C and three others of α giving a total of 15 different FVDS for training will be used to various sizes of dampers utilized in an RC structure while 3 different FVDS combinations for validating will be performed. The values of C were chosen based on the typical values of C used in such RC structures that can be found in the literature or by means of iteration [79, 80].

Table 3: Combinations of C and α used in the analyses for Training

Model No.	α	C (kN.sec/m)
1	0.3	500
2	0.3	800
3	0.3	1500
4	0.3	2000
5	0.3	2700
6	0.5	500
7	0.5	800
8	0.5	1500
9	0.5	2000
10	0.5	2700
11	1	500
12	1	800
13	1	1500
14	1	2000
15	1	2700

Table 4: Combinations of C and α used in the analyses for Validating

Model No.	α	C (kN.sec/m)
1	0.3	500
2	0.5	500
3	1	500

3.6 Artificial Neural Network

Artificial intelligence as multidisciplinary combining disciplines such as information theory, computer sciences, neurophysiology and etc. has been progressed since 1956. The main and fundamental objective of this multidisciplinary is to replicate and perform tasks or make decisions in a similar manner to how the human brain does. The artificial intelligence has gained both popularity and importance due to its ability to solve problems or do very complex calculations or estimations with very high efficiency and accurateness similar to what experts do or even better. Thus, artificial intelligence started to be implemented and incorporated in the field of civil engineering including multi-objective shape control, self-diagnosis, and reinforcement learning procedures [81]. Furthermore, artificial intelligence can be used to estimate

the compressive strength of conventional and high strength self-consolidating concrete or high strength concrete incorporated with high volume fly ash [82] or evaluate slope failure [83]. Moreover, Das et al. [84] estimated the maximum dry density and unconfined compressive strength of cement stabilized soil. Therefore, ANN technique was selected to establish an estimation model of the response of RC structures equipped with the size of FVD by using the results obtained from the nonlinear time history analysis (NTHA). The neural network training function that was used in this thesis was Levenberg-Marquardt backpropagation (trainlm) since it showed the best and most accurate results after investigating all other network training functions. The code adopted from Okoh [85] is explained in Appendix A and is used for determining the best number of hidden layers and neurons in terms of the performance. Furthermore, a code was written to determine the fitting rate or R^2 and Root mean square error (RMSE) and plot the findings. The results showed a good agreement between the code and neural network tool in MATLAB. The following tables show the neural network training function, the number of hidden layers, and the number of neurons that were used for establishing the prediction model of each response as an envelope and in the time domain.

Table 5: The Properties of Neural Network Training Function Used in Prediction in Time Domain

	Training Function Used	No. of Hidden Layers	No. of Neurons
Acceleration	Levenberg-Marquardt backpropagation	5	50
Displacement		5	50

Table 6: The Properties of Neural Network Training Function Used in Prediction of Peak (Envelope) Responses

Response Type	Training Function Used	No. of Hidden Layers	No. of Neurons
Roof Acceleration		3	20
Inter-Story Drift Ratio		3	20
Input Energy	Levenberg-Marquardt backpropagation	4	20
Damping Energy		2	20
Base Shear		2	20

Chapter 4

RESULTS AND DISCUSSION

4.1 Introduction

This chapter is devoted to discussing the results of structural analysis and ANN. Nowadays, scientists and engineers are using NTHA for designing and investigating the behavior of RC structures utilizing FVDs. In general, to design such complex structures an iterative approach, Figure 8, is being adopted by trying several properties of fluid viscous dampers, different values of both C and α, to obtain both a suitable structural response that meets the code requirements and economic system that can be practically installed to the bare RC structure. Thus, it can be observed that the deficiency in the conventional design method is its take requirements due to the fact that the engineer or researcher needs to repeat the entire NTHA for each earthquake record again once the damper properties are changed for the new iteration. As mentioned previously, this study is proposing novel prediction approaches based on ANN for fast estimation of low-, low-to-mid-, and mid-rise RC structures equipped with FVDs. This method can reliably be used as an alternative way to significantly reduce the time needed for analyzing and eventually designing such a building. The following sections will discuss preliminary results that were used in developing the prediction models. Furthermore, it will present the results of a comprehensive study to test and validate these models aiming to obtain a sufficient idea on their performance in different design scenarios.
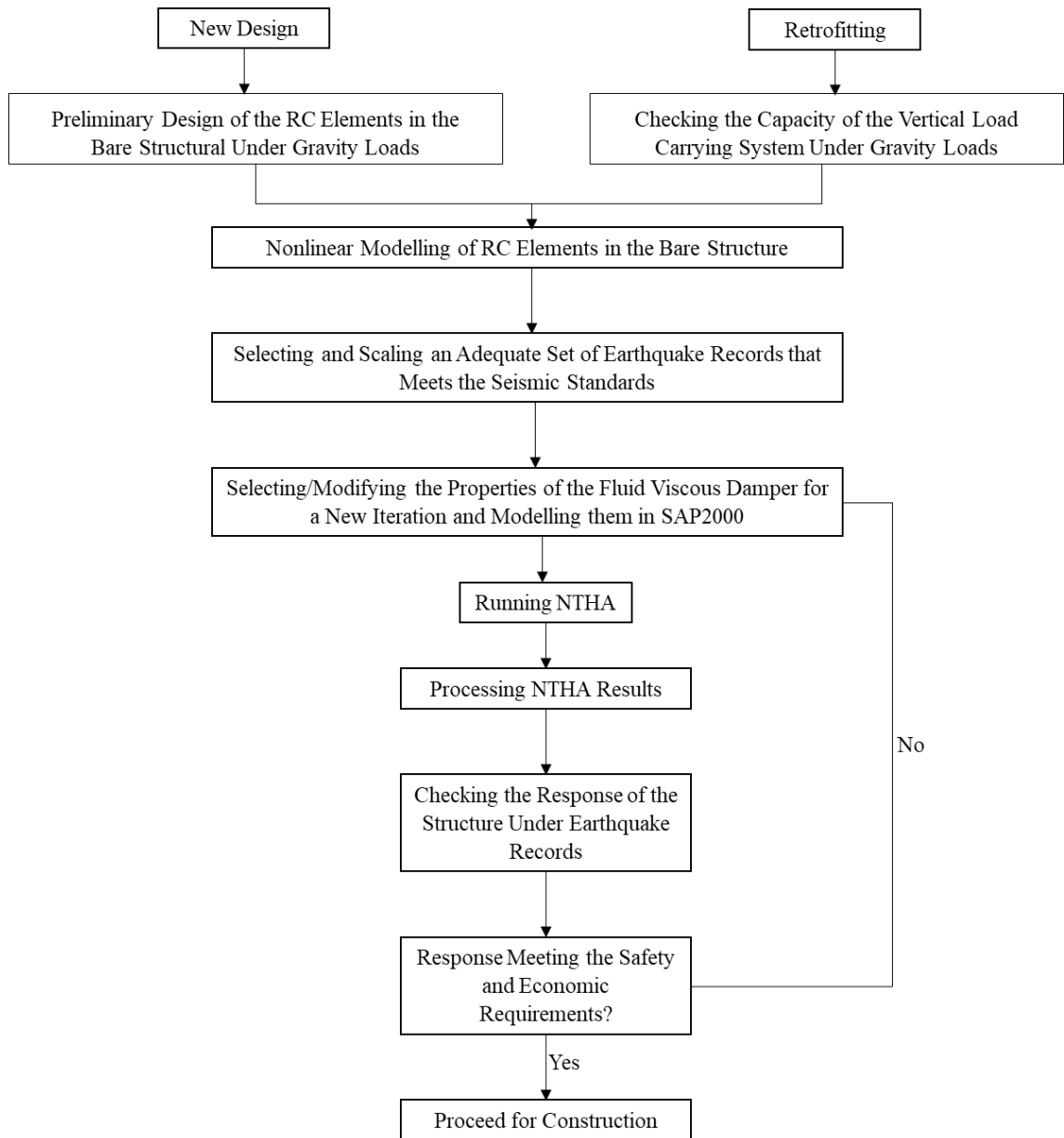
Figure 8: A framework generally used for conventional design/retrofitting process of RC structure with FVDs

4.2 Validating the Accuracy of the Finite Element Models

In this section, the validity of the method used for modeling the RC structures with FVDs using SAP2000 will be discussed. Generally, the results of the finite element models for a simple case 2D RC structural system is validated based on the previously available results from the literature [86]. Accordingly, the findings of the NTHA are plotted as shown in Figure 9. Figure 13 and Figure 14 show their trends considering

the effect of changing C and α properties of the damping device on the performance of the structure which is compared to previous findings in the literature. The values in Figure 9 are the average of the 18 earthquakes responses for the 3-story structure used in the study.
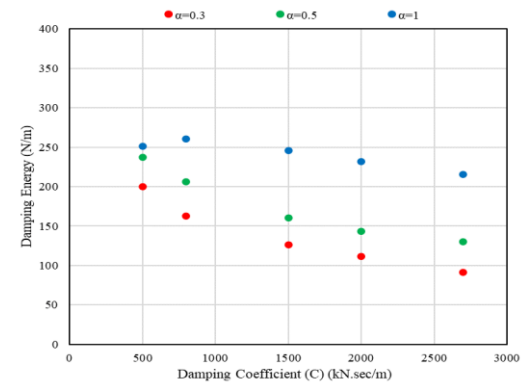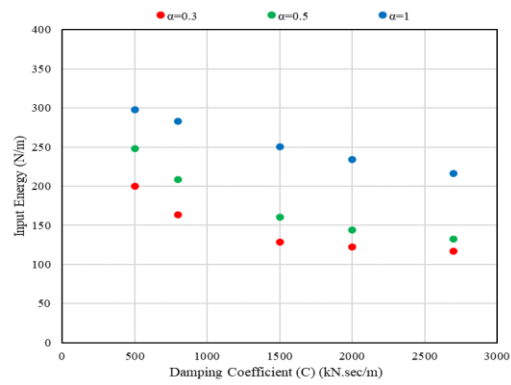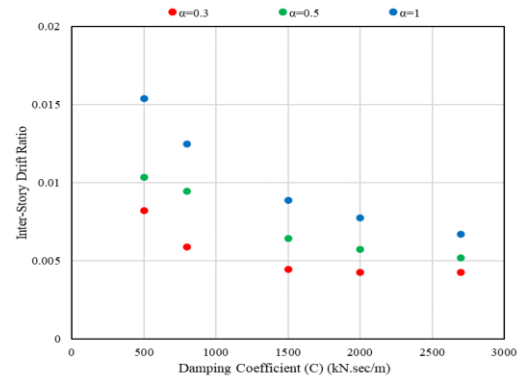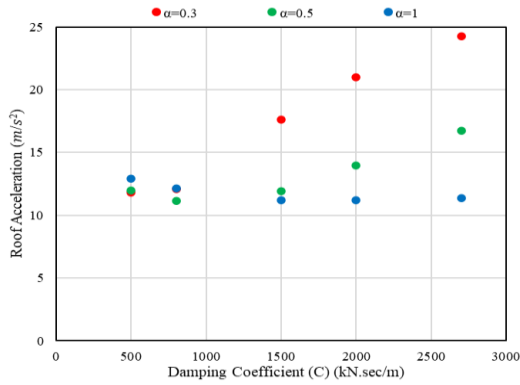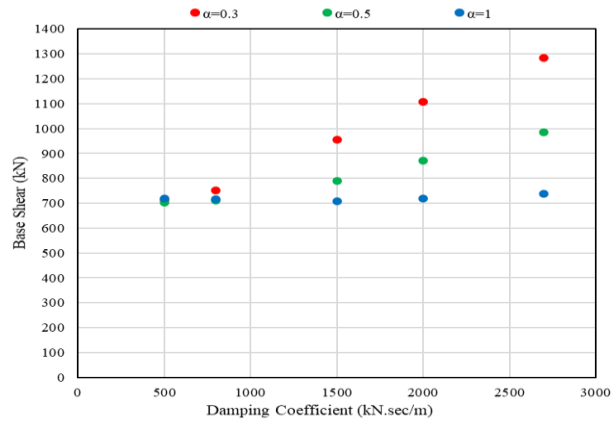
Figure 9: Trending of the results of the finite element models for three story
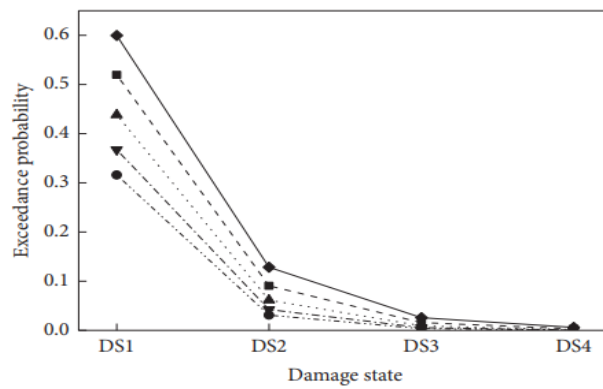
(a)
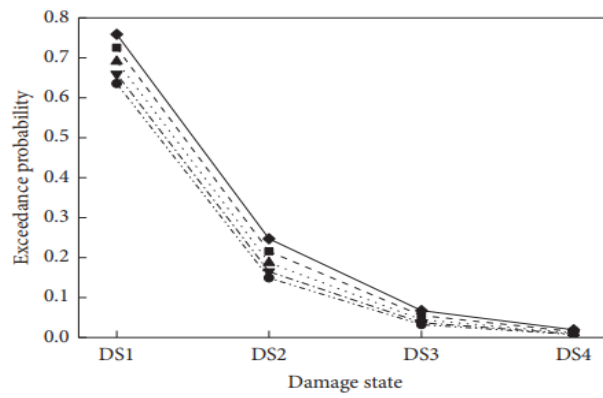
Figure 10: Roof acceleration for C values of 50 and 100 from Wei et al. [86]
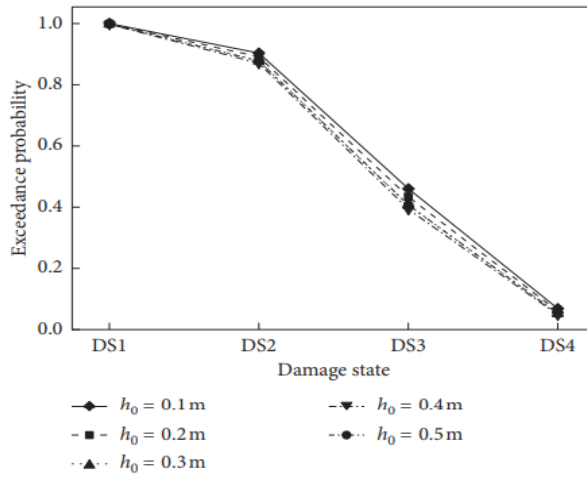
(a)
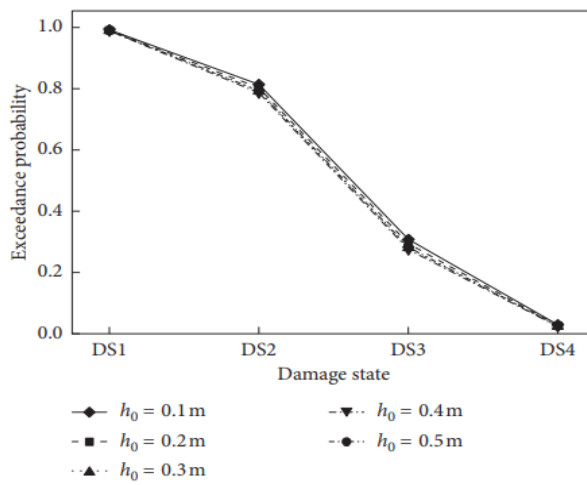
Figure 11: Peak relative displacement for C values of 50 and 100 from Wei et al. [86]
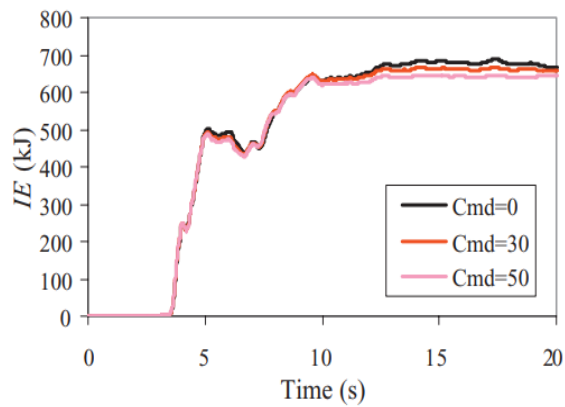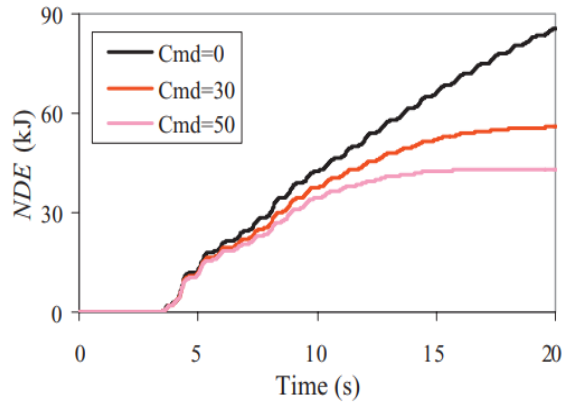
Figure 12: Input and natural damping energies for different values of C for Wong [25]

As shown in the figures above, the results are in consistent with the results of Wei et al. [86] where they concluded that the roof acceleration and peak relative displacement are irreconcilable since roof acceleration increases as the C increases while peak displacement decreases at high Cs leading to a very difficult design process represented by problem in finding a balanced design with both minimum acceleration and displacement responses. While input and damping energies results are in consistent with findings of Wong [25].
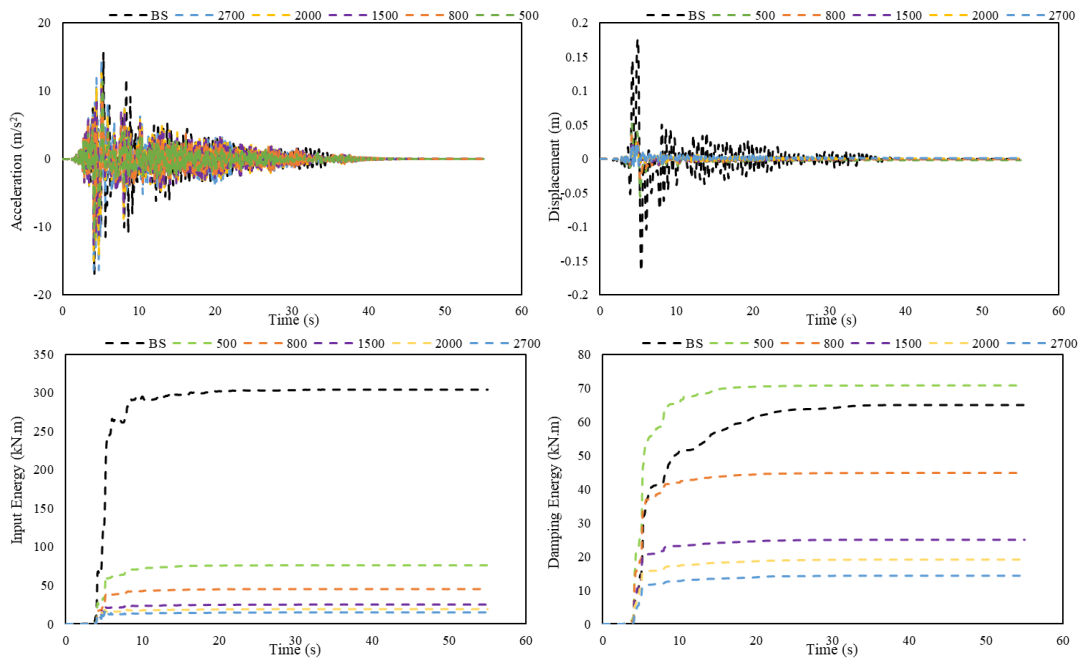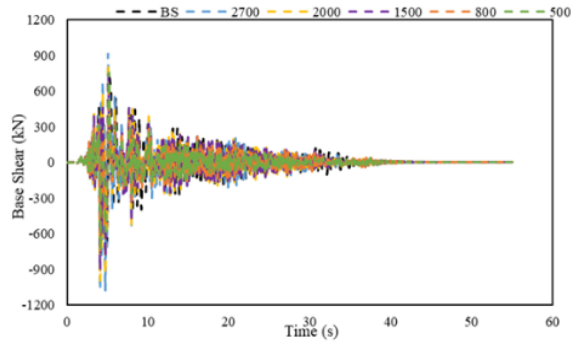
Figure 13: Validating the results of the finite element models in the time domain for different C values for Imperial Valley-06 (171) earthquake an example of three story

As C increases, the acceleration in time domain increases. In the contrast, the increase of C results in reduction in the displacement in time domain. This finding is consistent with the results of Wei et al. [86]. Moreover, the results of the input and damping energies are consistent with other studies such as Wong [25] where it can be observed that as the C increases, input and damping energies decrease as illustrated in Figure 9 and Figure 13.

36
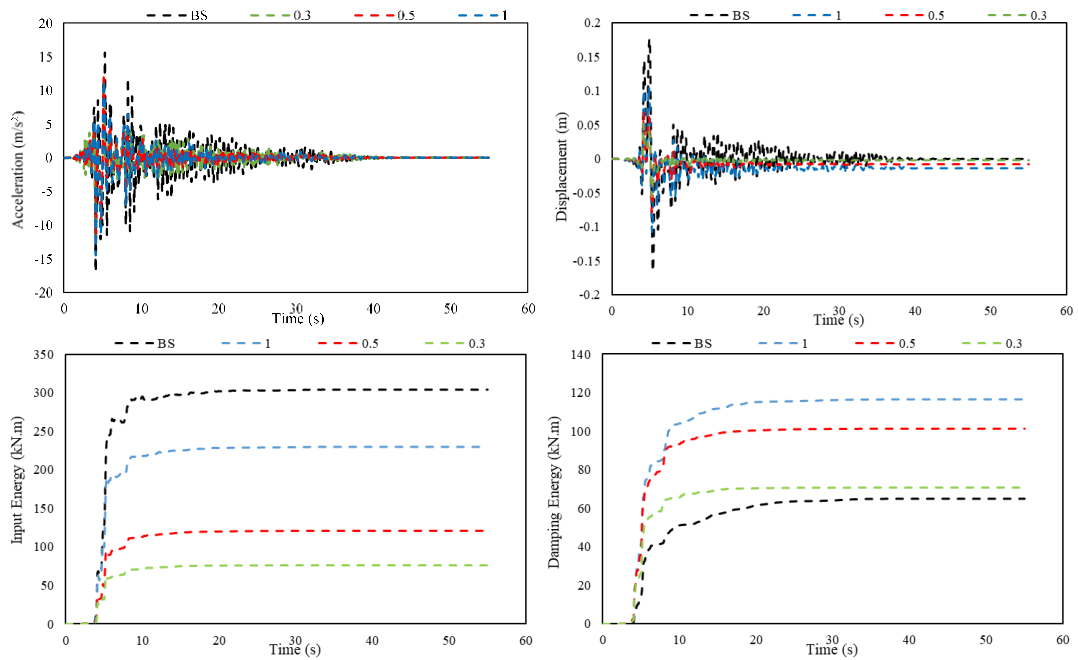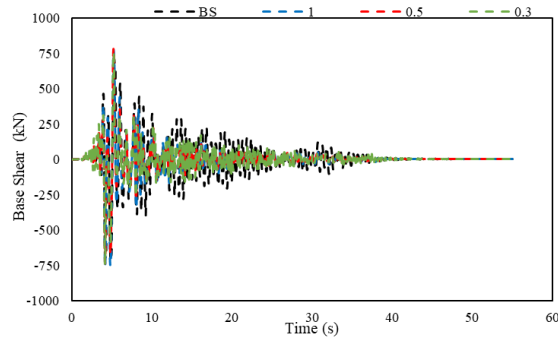
Figure 14: Validating the results of the finite element models in the time domain for different α values for Imperial Valley-06 (171) earthquake an example of three story

Figure 14 illustrates the effect of α on the acceleration and displacement in the time domain. It can be seen that α=1 exhibited the highest reduction in acceleration while for displacement, α=0.3 showed the lowest result in comparison to α=0.5 and α=1. However, the acceleration response of the three cases is almost the same whereas, for displacement, the α =0.3 exhibited a huge superior performance compared to the other cases. These findings are consistent with the results of Ras and Boumechra [41]. On the other hand, in terms of α effect on the input and damping energies, α is linearly proportional to the input and damping energies so as α decreases, input and damping energies decrease too. Furthermore, as can be seen in Figure 14, the effect of α on the base shear is very minor or even does not exist for all values α [87, 88]. Based on these results, FVD with α=0.3 (nonlinear) gives the lowest energy responses and hence, the best performance. In addition to that, the best properties of FVD in order to possess the best performance and reduce the structure responses are α with lower nonlinear value and higher C.

4.3 Proposed Models

In practice, two different methods of reporting the results of NTHA are being used in the literature. These methods are mainly the response in the time domain and the absolute peak response of the structure under a given ground motion record. Each of

37

these methods has its own use. The time domain approach is generally preferred by those who are willing to understand the behavior of a structure under a single or a low number of earthquake events. Whereas, the peak one is mainly used in designing and investigation phases where a high number of ground motion records are processed. Accordingly, this study will propose two different prediction approaches for estimating the peak response of the structure and the response under a single even in the time domain. These will be done through a numerical investigation taking the results of about 2500 NTHAs being conducted for 72 different RC structures to provide a solid prediction model with high accuracy.

4.4 Prediction in the Time Domain

In this section, the prediction in time domain will be discussed.

4.4.1 Proposed Algorithm

The intention in providing an estimation model for the response of a viscously damped structure in the time domain is to reduce the time required for estimating models. Accordingly, the algorithm of handling a prediction task using the proposed algorithm in this study is compared to the approach generally used in direct integration nonlinear response history analysis.

Algorithm of NTHA

Select and Scale an Earthquake Records	Define (C and α)	Obtain the Response of the Bare Structure

Predicting the Structural Responses
(After training the system and saving it, the prediction take below 2 minutes)

Processing the Results of the NTHA

Proposed ANN Algorithm
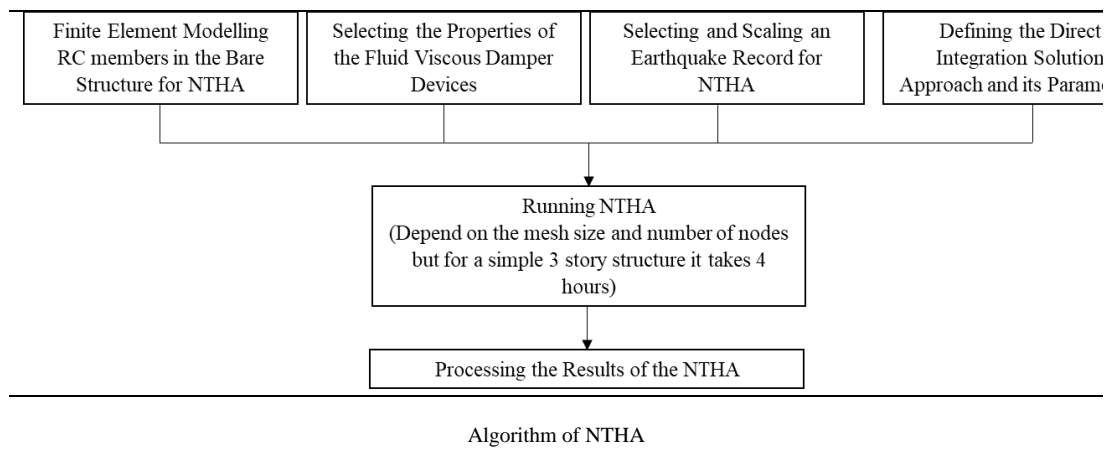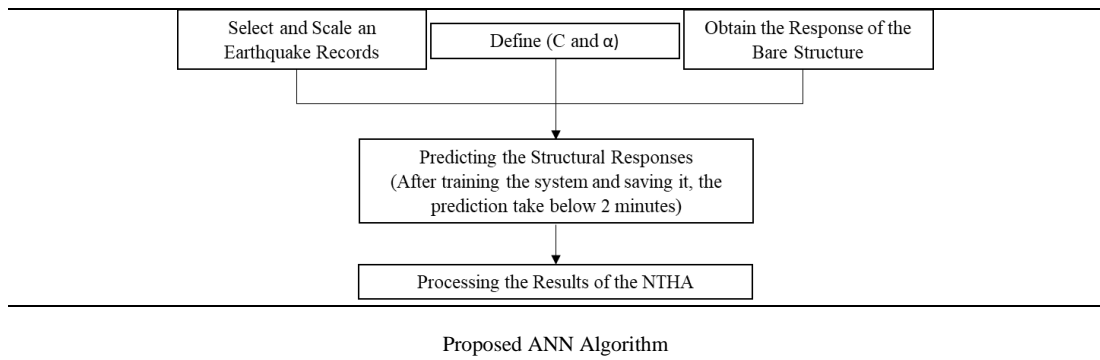
Figure 15: Comparison between the proposed algorithm in ANN and the NTHA one

As shown in Figure 15 the estimation method can be considered as significantly improve one as compared to the conventional NTHA where it requires considerably lower number of inputs and lesser time.

4.4.2 Proposed ANN Configurations

In order to obtain good estimation accuracy, the scaled ground acceleration, ground velocity, ground displacement, ratio of ground acceleration to ground velocity (representing the frequency content at a certain time), and a time step of earthquake record in addition to the response of bare structure (same response type as the intended one), C, and α values are used as an input to the ANN. Furthermore, 50 neurons for each of the 5 hidden layers are utilized for training the prediction model using trainlm method to handle the solution of the feedforward backpropagation network in MATLAB. A graphical summary of the two configurations one acceleration and another for the displacement are shown in Figure 16 illustrates the acceleration response in the time domain of four different setups. The first setup includes ground acceleration only. The second setup illustrates the use of ground acceleration and ground velocity in building the setup whereas the third setup shows the response of using ground acceleration, ground velocity, and ground acceleration to ground velocity ratio. Finally, the last setup is built with all previously mentioned ground

responses plus the ground displacement. As can be seen from the figure, implementing all ground responses in the prediction of the acceleration in time domain showed the best and superior result in comparison to include some of the ground response. This can be attributed to the fact that the last setup of all ground responses expresses the full and complete behavior of the earthquake which results in the best accuracy and performance. Figure 17 shows the same process for predicting the displacement in the time domain. These results allow us to identify the most important earthquake parameters in order to be used in developing the prediction model and thus, based on the results in Figure 16 and Figure 17, all ground responses will be used in building the prediction model to guarantee the best performance and accuracy.

Loma Prieta (RSN 802)

Ground Acceleration	Ground Velcoity

Ratio of Ground Acceleration to ground Velocity	Ground Displcement
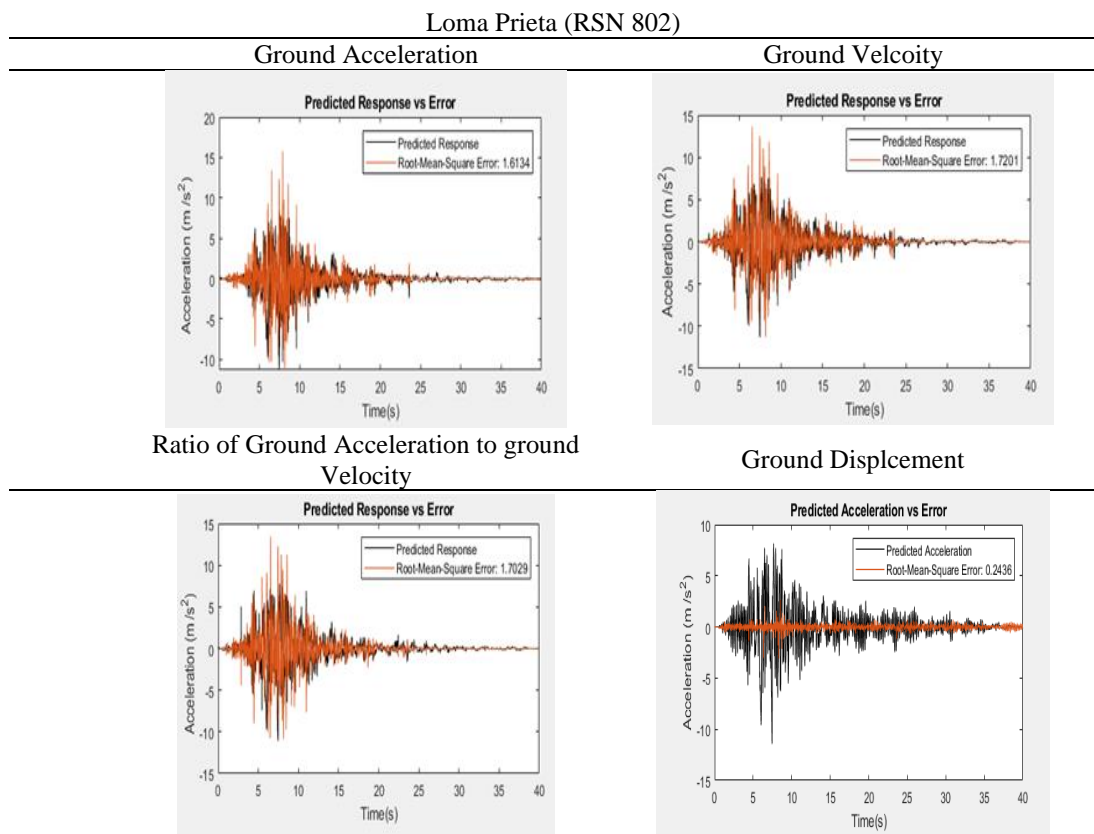
Figure 16: The acceleration response in time domain for different input parameters

Ground Acceleration	Ground Velcoity

Ratio of Ground Acceleration to ground Velocity	Ground Displcement
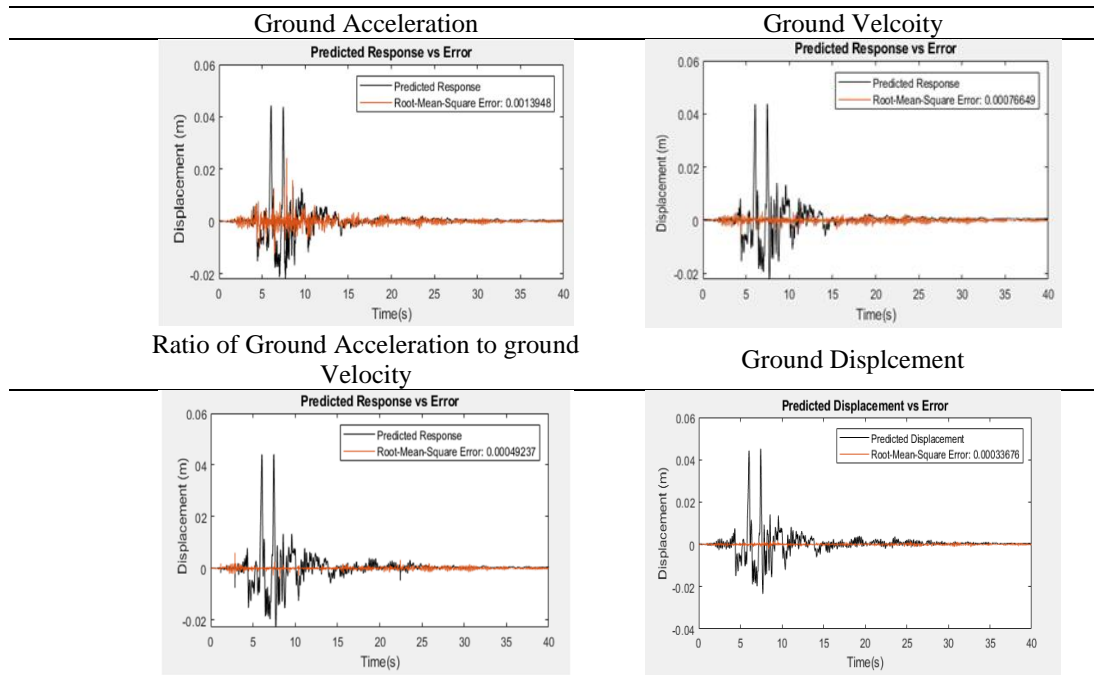
Figure 17: The displacement response in time domain for different input parameters
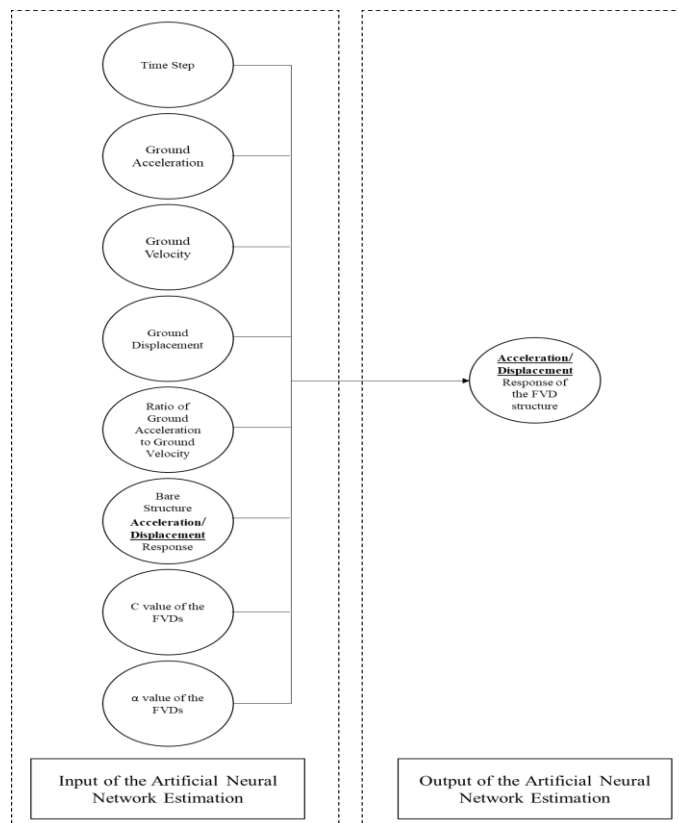
Figure 18: Proposed ANN algorithm for the response (acceleration and displacement) prediction in the time domain

4.4.3 Performance of this Method to Various Damper Properties

In this section, the performance of the proposed artificial neural network method to different fluid viscous dampers by means of various C and α values used for developing the model will be investigated comprehensively for the case of Loma Prieta (RSN 802). The purpose behaind selecting this earthquake is that it provides a high magnitude (6.93 Mw) and high PGA value (0.514 g) with the properties of pluse-like that as discussed previously gives the most destructive energy for RC structures. To be able to determine the effect of using FVD on the acceleration and displacement responses in the time domain.
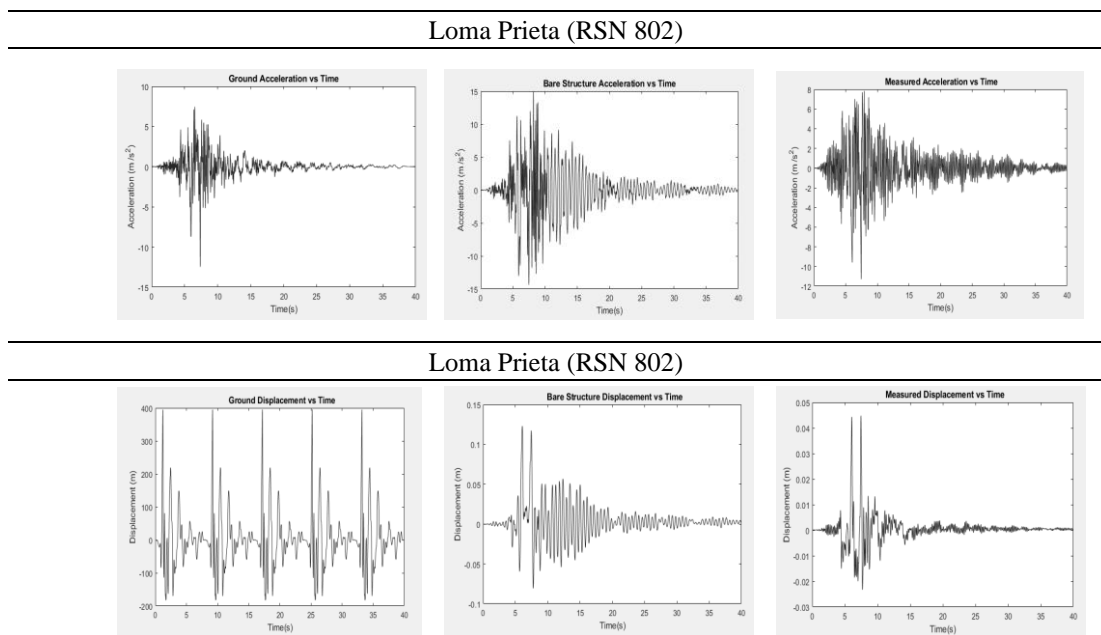
Figure 19: The effect of using FVD on the responses (acceleration and displacement) of the structure

As can be seen from the figure above, the usage of FVD shows a good result in significantly reducing the responses (acceleration and displacement) of the structure. On the other hand, a code was written using MATLAB to plot the prediction responses, fitting rates, and the errors which is included in Appendix B. The first row represents the acceleration response in the time domain whereas the second one

represents the displacement response. Moreover, Figure 20 shows the prediction model for acceleration in the time domain.
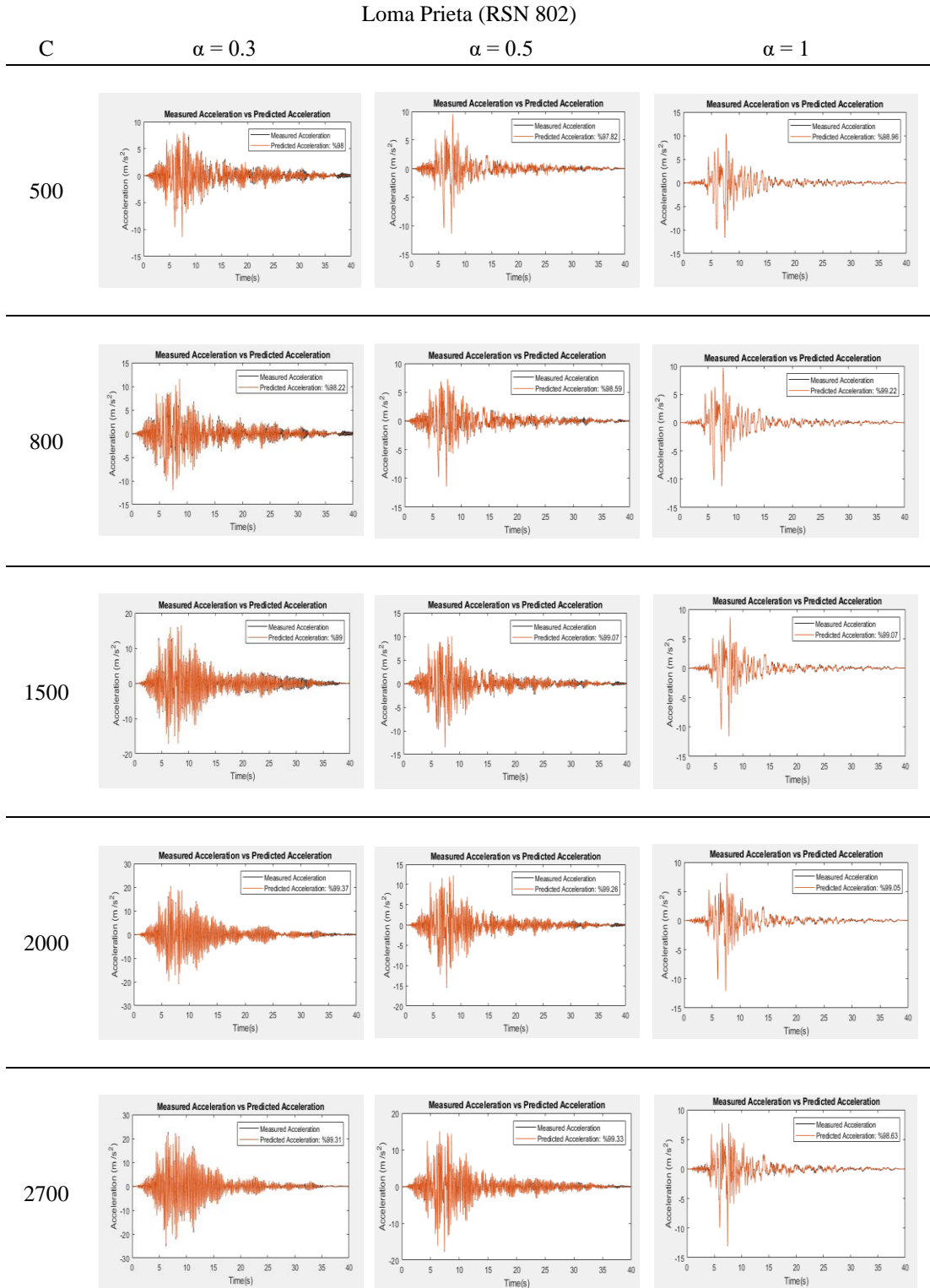
Figure 20: Acceleration prediction in the time domain an example of the case of three story

	Loma Prieta (RSN 802)		
C	α = 0.3	α = 0.5	α = 1
500			
800			
1500			
2000			
2700			

	Loma Prieta (RSN 802)		
C	α = 0.3	α = 0.5	α = 1
500			

800			
1500			
2000			
2700			

Loma Prieta (RSN 802)

C	$\alpha = 0.3$	$\alpha = 0.5$	$\alpha = 1$
500			
800			
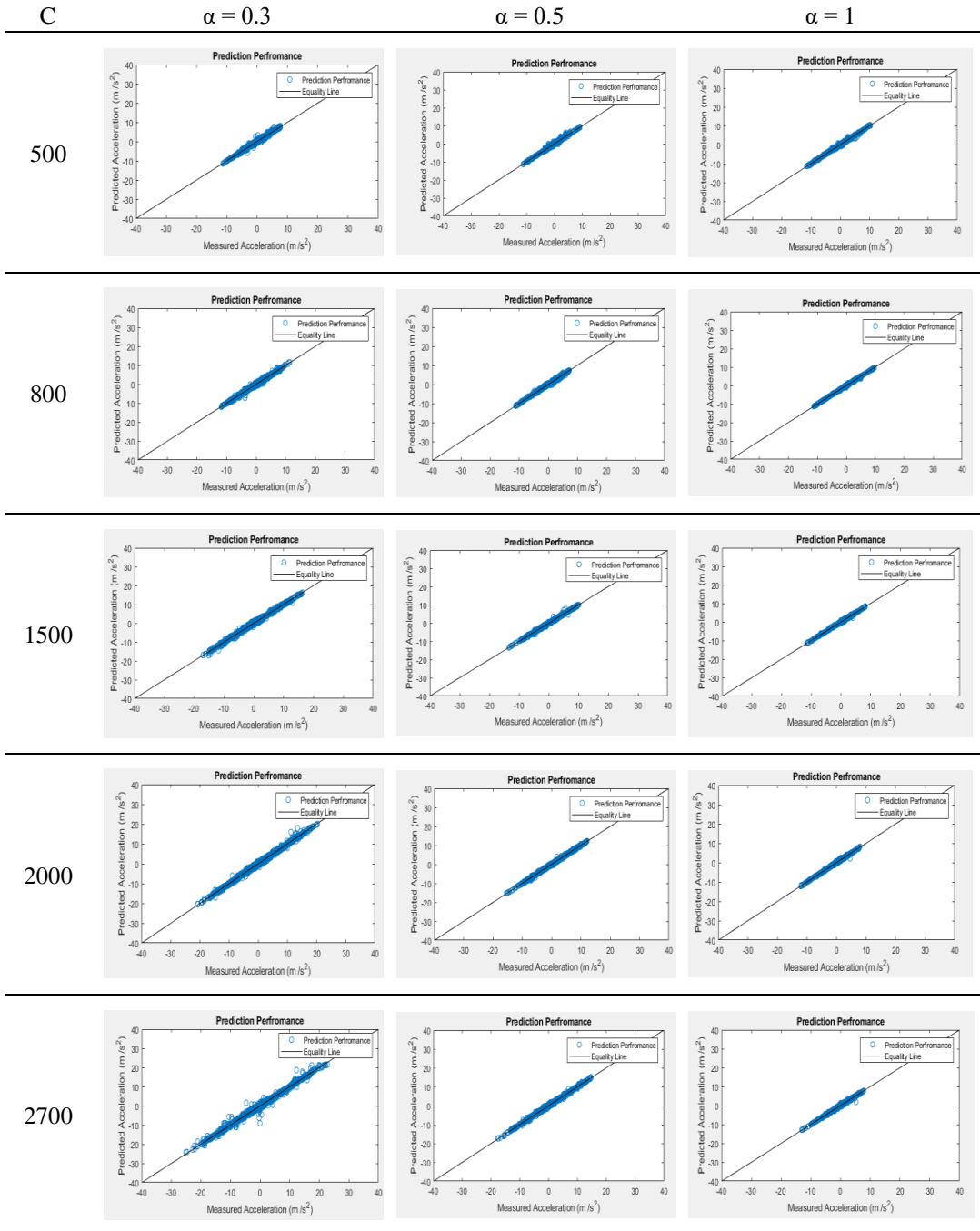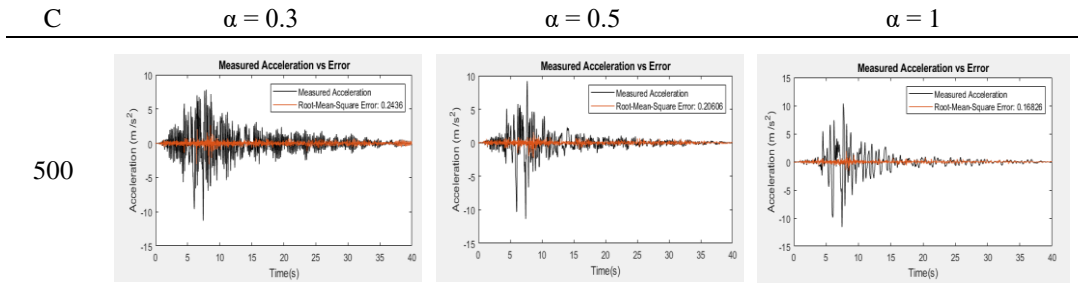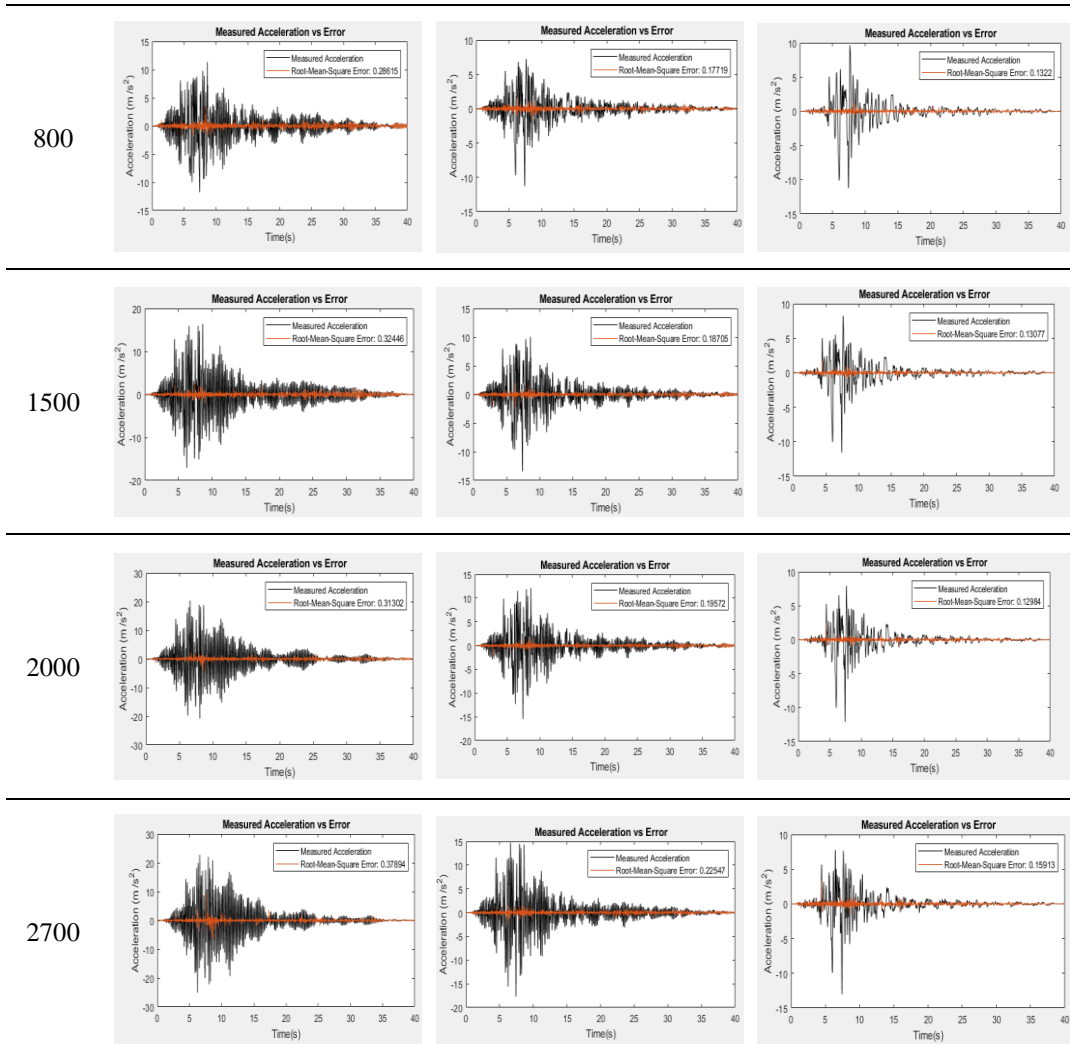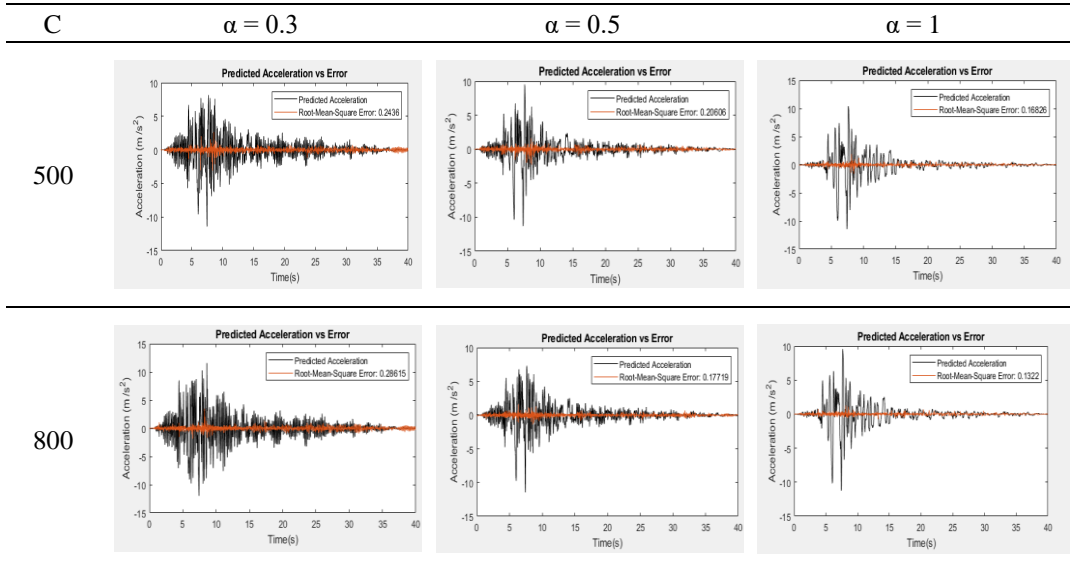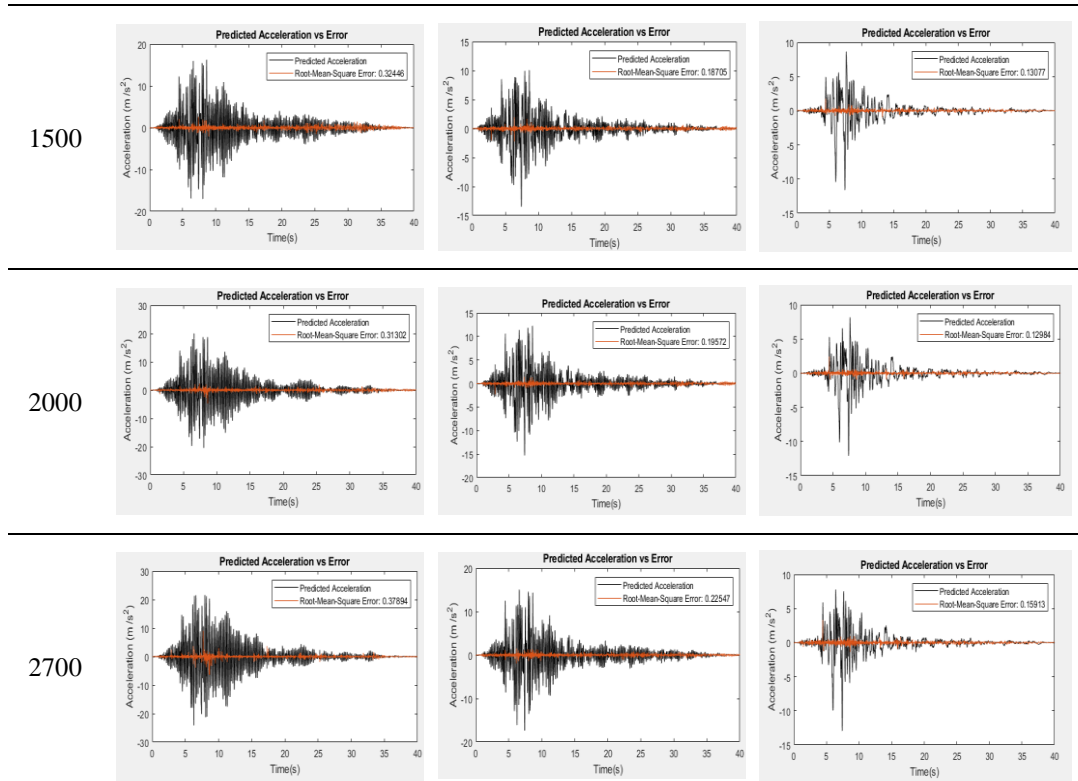
Figure 21: Performance of the proposed model for acceleration in time domain for an example of the case of three story

The prediction of the acceleration in the time domain was performed to investigate the applicability of ANN in predicting the response in the time domain. The results in Figure 20 indicate that ANN is capable of accurately predicting the acceleration in the time domain of earthquakes with an R^2 value of 0.9954 which can give a high sense of accuracy. As can be observed from Figure 21, the RMSE is 0.37894 which is acceptable since the limit is 0.5.

Loma Prieta (RSN 802)			
C	$\alpha = 0.3$	$\alpha = 0.5$	$\alpha = 1$
500			
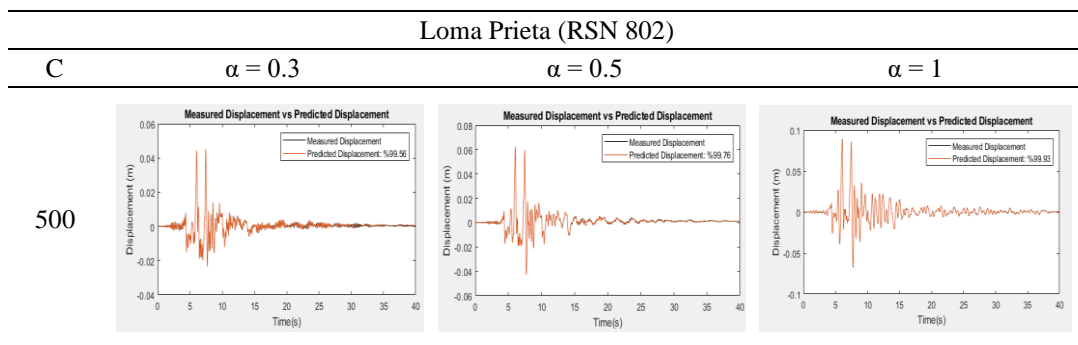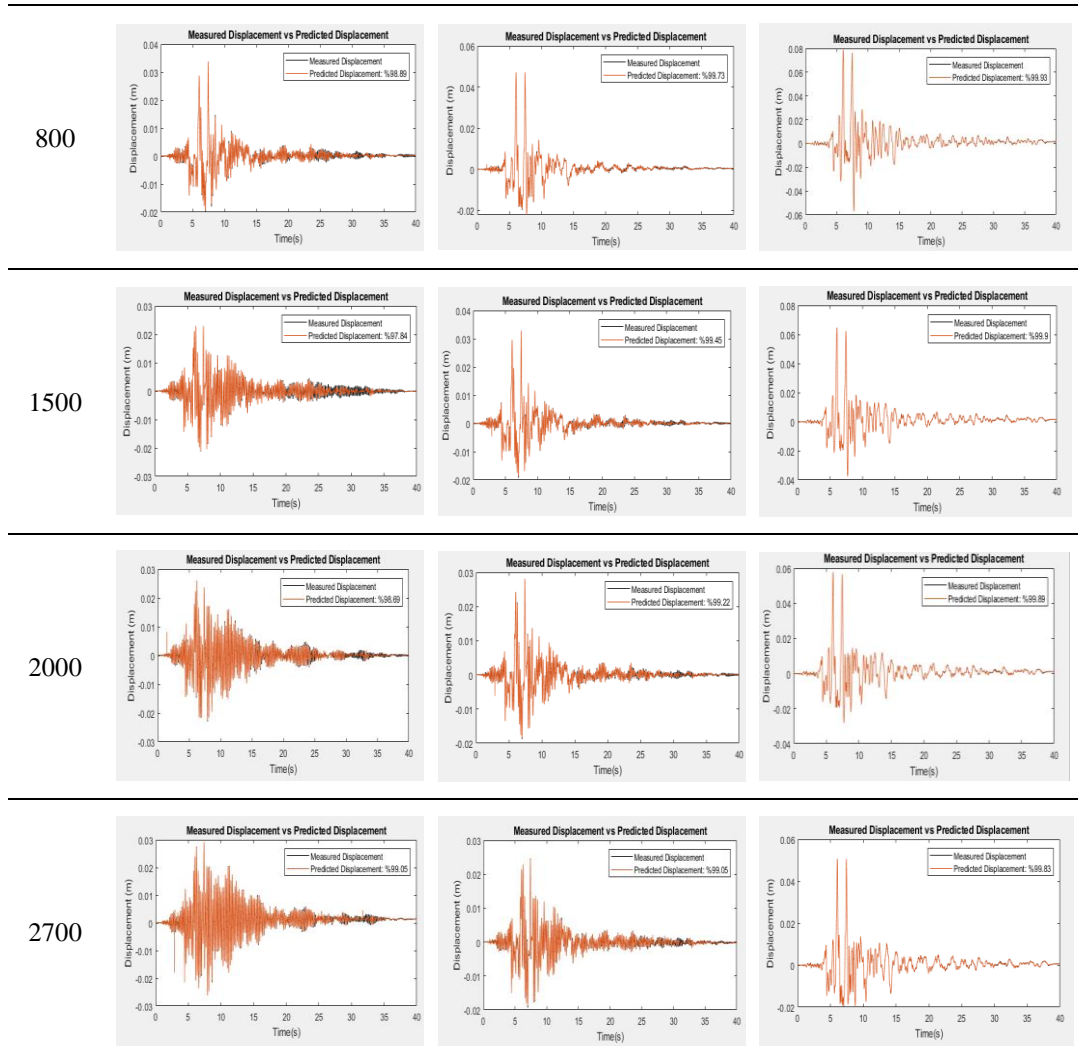
Figure 22: Displacement prediction in the time domain an example of the case of three story

	Loma Prieta (RSN 802)		
C	α = 0.3	α = 0.5	α = 1
500			
800			

1500			
2000			
2700			

Loma Prieta (RSN 802)

C	α = 0.3	α = 0.5	α = 1
500			
800			
1500			

2000			
2700			

Loma Prieta (RSN 802)

C	α = 0.3	α = 0.5	α = 1
500			
800			
1500			
2000			
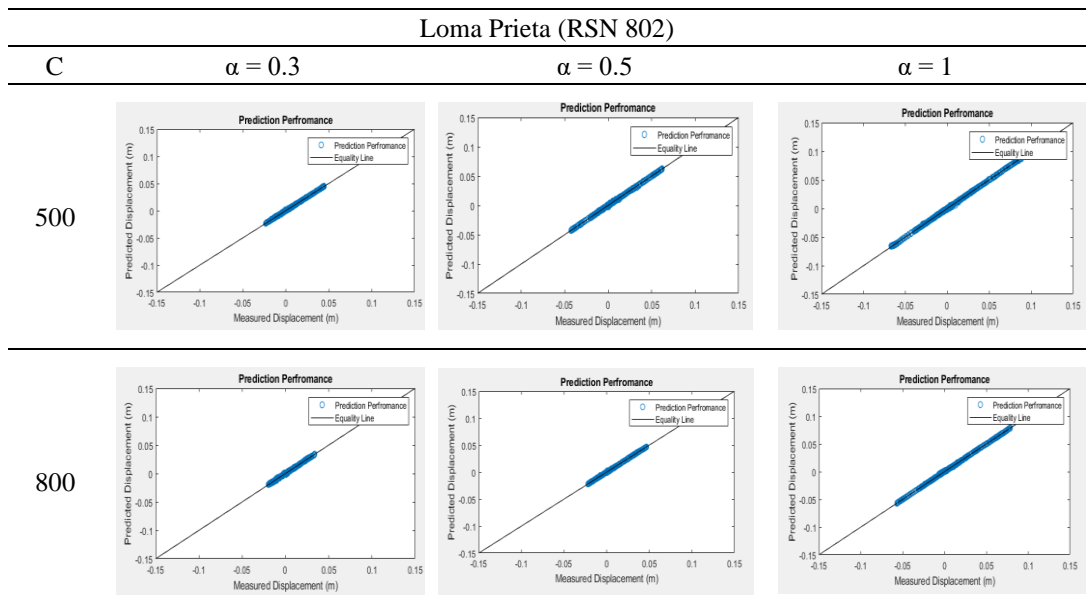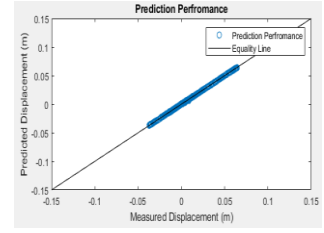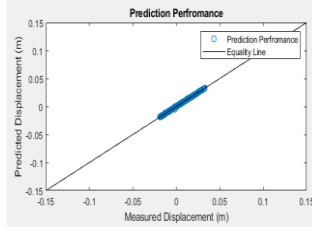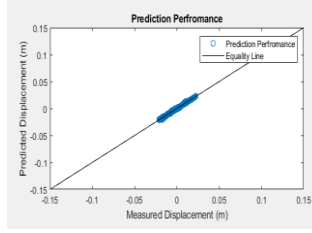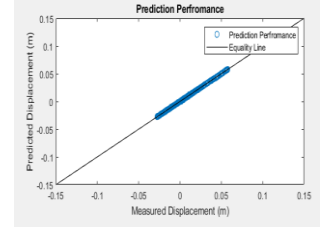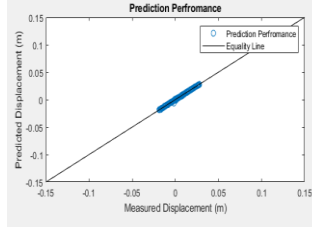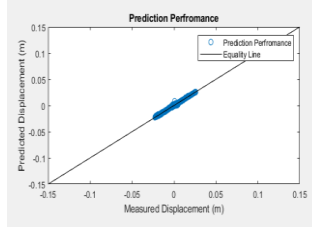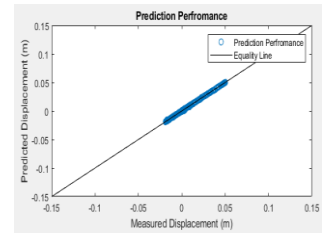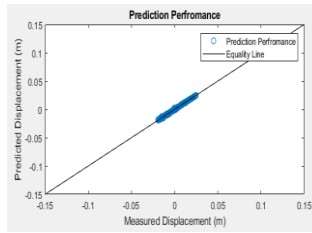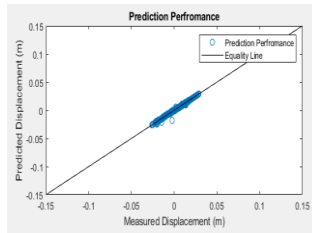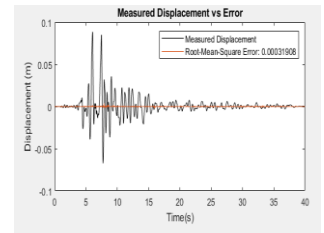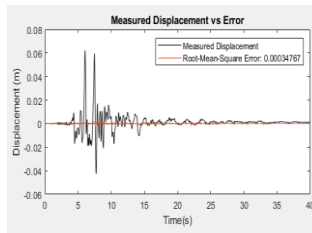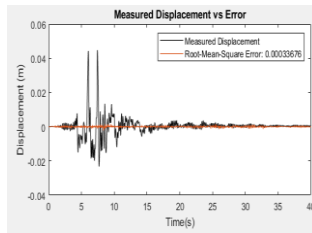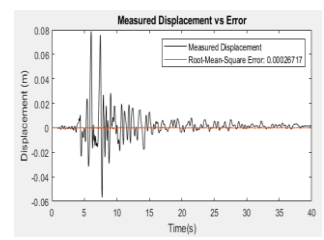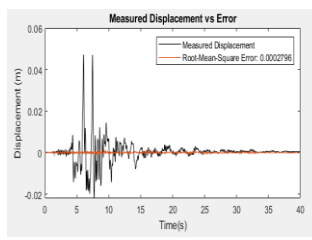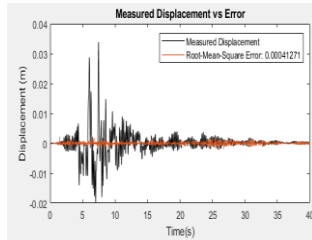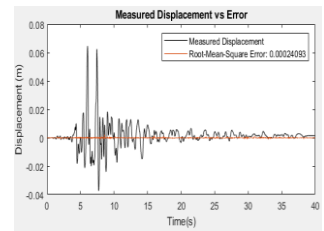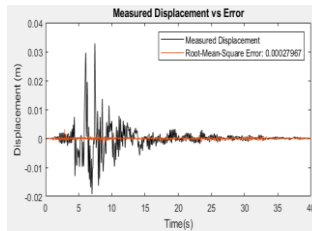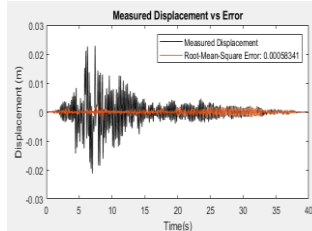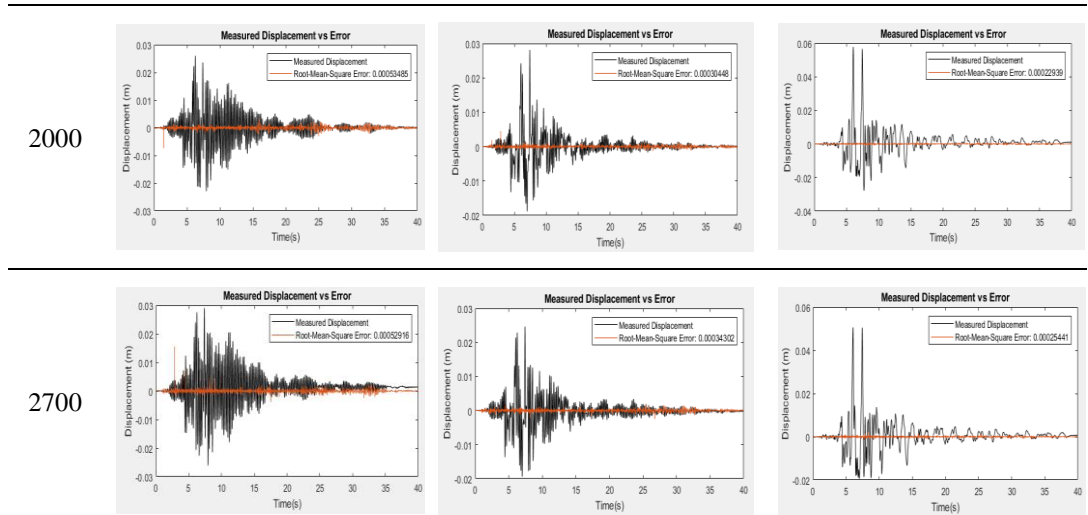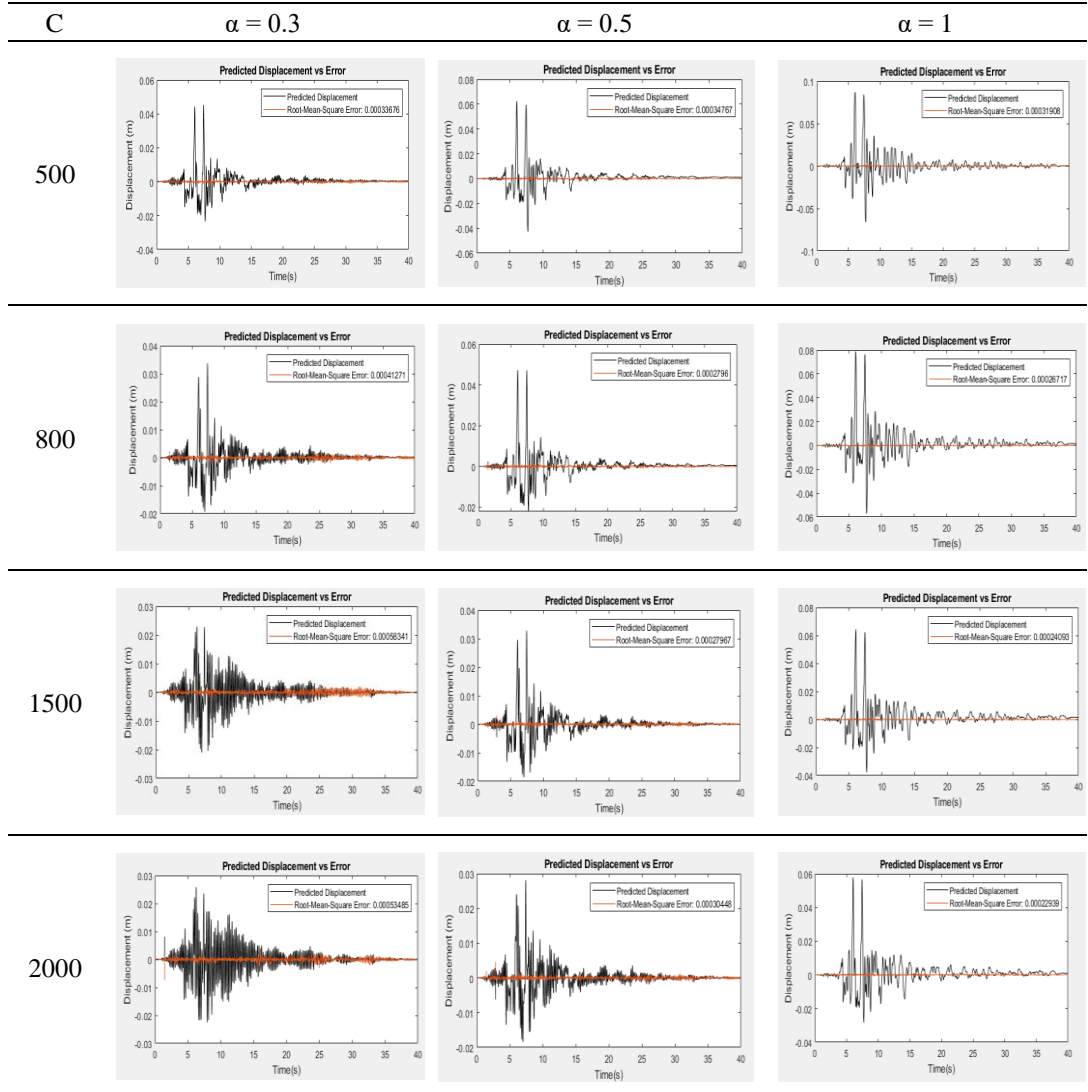
| 2700 | |
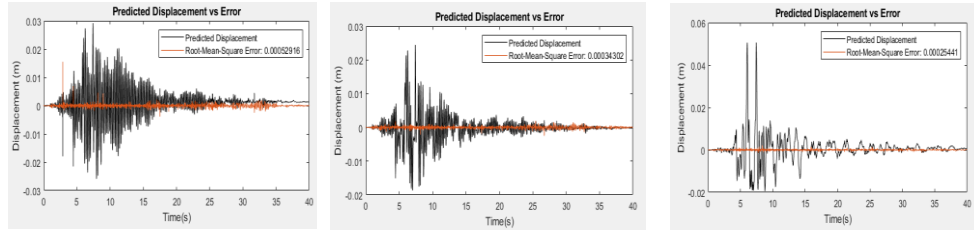
Figure 23: Performance of the proposed model for displacement in time domain for an example of the case of three story

The prediction of the displacement in the time domain was performed to investigate the applicability of ANN in predicting the response in the time domain. The results in Figure 22 indicate that ANN is capable of accurately predicting the displacement in the time domain of earthquakes with an R^2 value of 0.99834 which can give a high sense of accuracy. As it can be observed from Figure 23, the maximum RMSE is 0.00058 which is acceptable.

4.5 Applicability of Prediction Model to Different Types of Earthquake Records

As mentioned previously, for each earthquake records a separated trained network must be done prior to utilizing it for prediction. In this section, the suitability of the proposed ANN configuration for a different types of ground motions that were selected to cover a wide range of characteristics such a near fault, far fault, and pulse-like is investigated herein. For this reason, the response (acceleration and displacement) of an RC structure utilizing FVD with C (2700) and α (1) properties were predicted and compared against the results of NTHA as follows.

Chi-Chi, Taiwan (RSN 1182)	Imperial Valley-06 (RSN 171)	San Fernando (RSN 323)

Coalinga-01(RSN 295)	Imperial Valley-06 (RSN 160)	Coalinga-01(RSN 368)
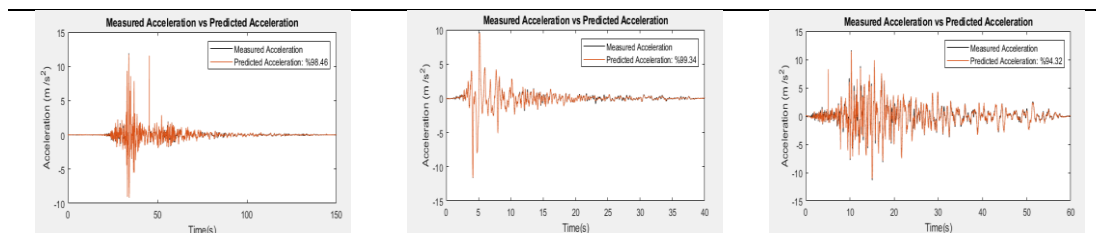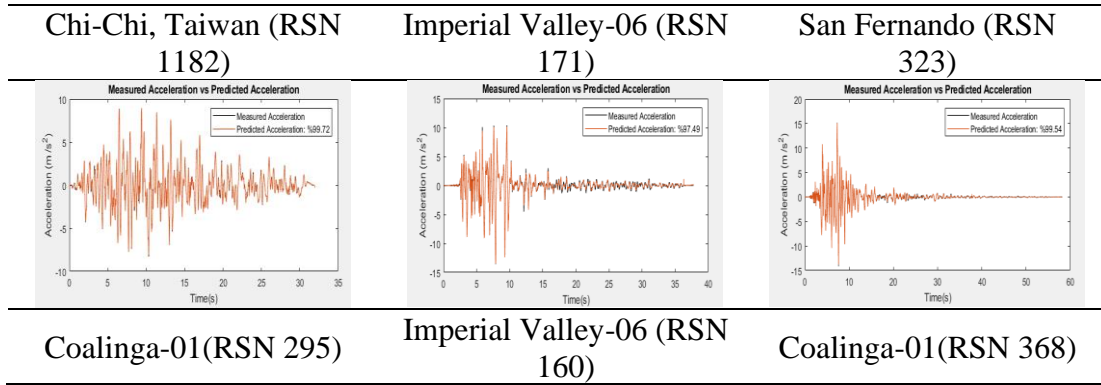
Figure 24: Applicability of the acceleration prediction in time domain for different types of earthquakes

Chi-Chi, Taiwan (RSN 1182)	Imperial Valley-06 (RSN 171)	San Fernando (RSN 323)

Coalinga-01(RSN 295)	Imperial Valley-06 (RSN 160)	Coalinga-01(RSN 368)

Chi-Chi, Taiwan (RSN 1182)	Imperial Valley-06 (RSN 171)	San Fernando (RSN 323)

Coalinga-01(RSN 295)	Imperial Valley-06 (RSN 160)	Coalinga-01(RSN 368)

51

| Chi-Chi, Taiwan (RSN 1182) | Imperial Valley-06 (RSN 171) | San Fernando (RSN 323) |
| Coalinga-01(RSN 295) | Imperial Valley-06 (RSN 160) | Coalinga-01(RSN 368) |
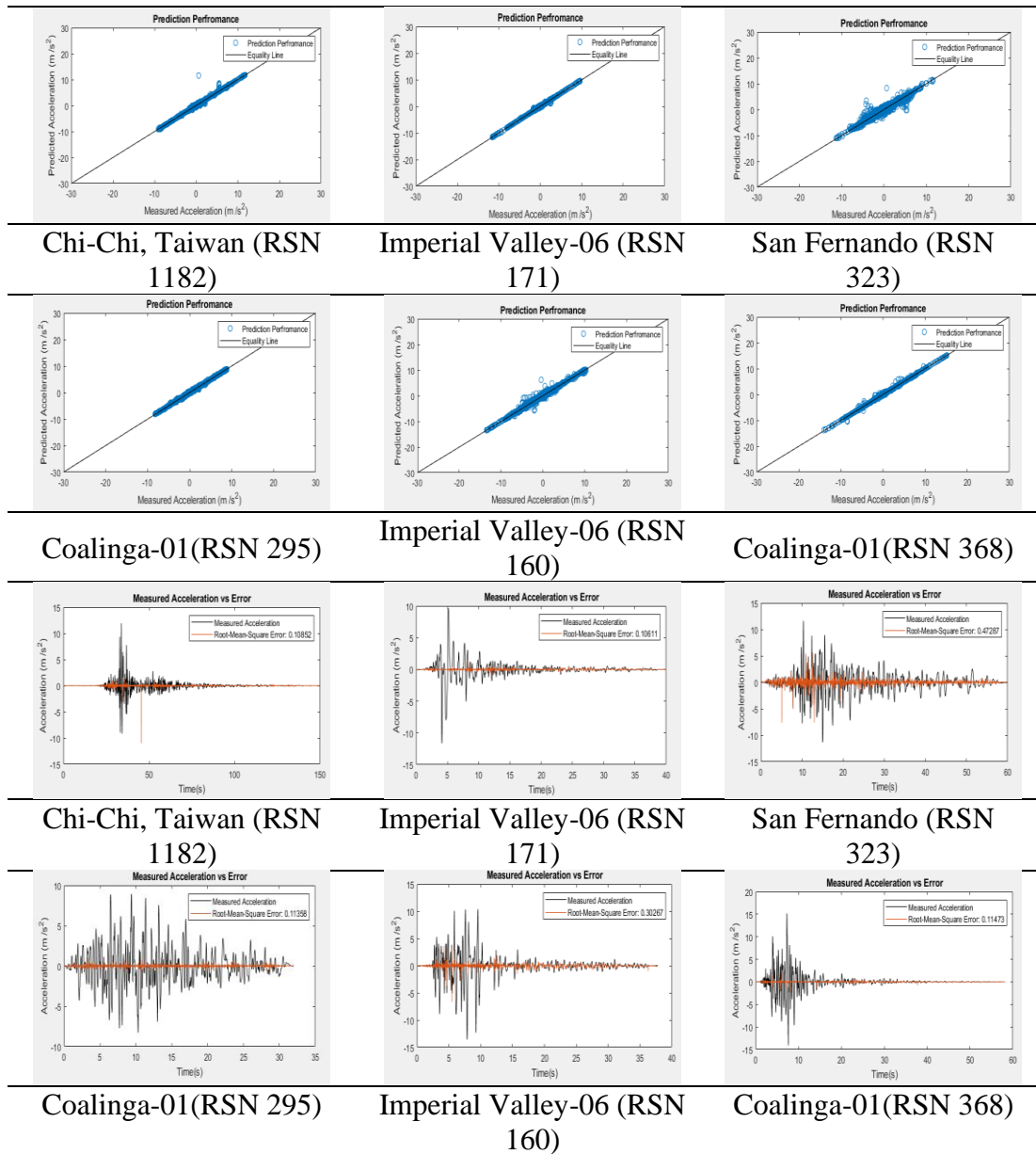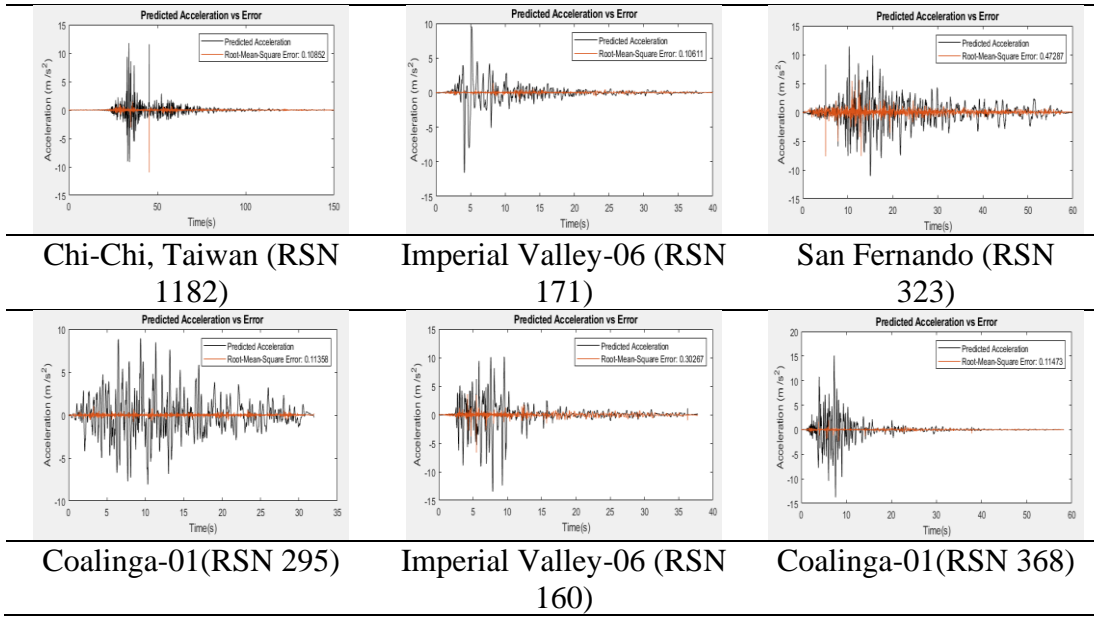
Figure 25: Validation of the proposed model for acceleration in time domain for different types of earthquakes

As it can be observed from Figure 25, the maximum RMSE is 0.47287 which is acceptable since it is less than 0.5.

| Chi-Chi, Taiwan (RSN 1182) | Imperial Valley-06 (RSN 171) | San Fernando (RSN 323) |
| Coalinga-01(RSN 295) | Imperial Valley-06 (RSN 160) | Coalinga-01(RSN 368) |
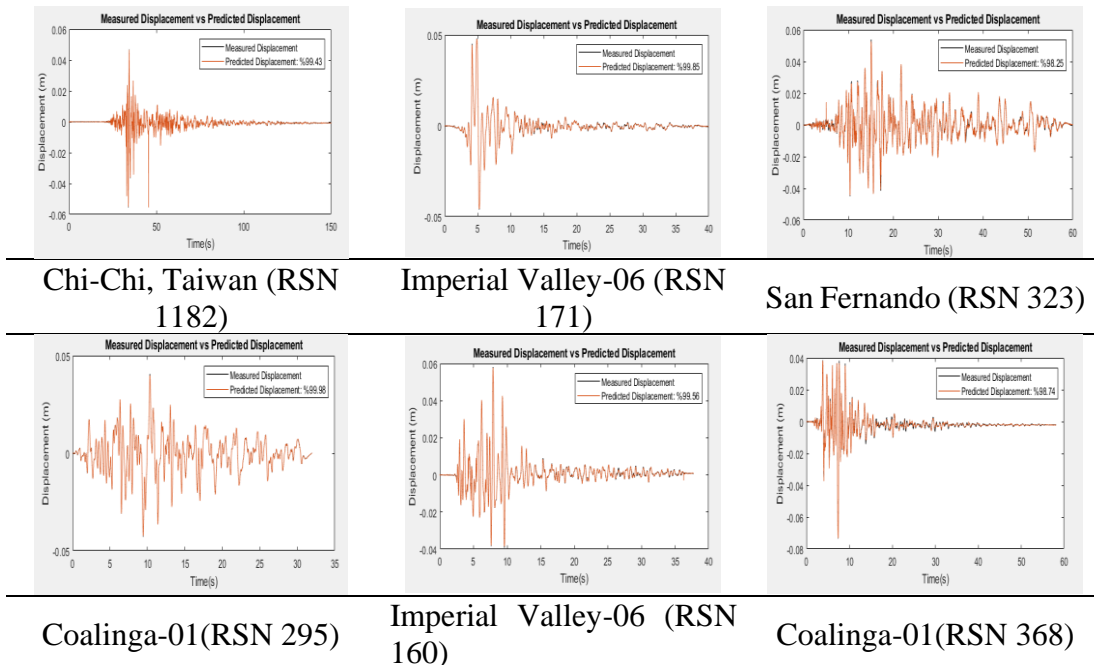
Figure 26: Applicability of the displacement prediction in time domain for different types of earthquakes

Chi-Chi, Taiwan (RSN 1182)	Imperial Valley-06 (RSN 171)	San Fernando (RSN 323)
Coalinga-01(RSN 295)	Imperial Valley-06 (RSN 160)	Coalinga-01(RSN 368)
Chi-Chi, Taiwan (RSN 1182)	Imperial Valley-06 (RSN 171)	San Fernando (RSN 323)
Coalinga-01(RSN 295)	Imperial Valley-06 (RSN 160)	Coalinga-01(RSN 368)
Chi-Chi, Taiwan (RSN 1182)	Imperial Valley-06 (RSN 171)	San Fernando (RSN 323)
Coalinga-01(RSN 295)	Imperial Valley-06 (RSN 160)	Coalinga-01(RSN 368)
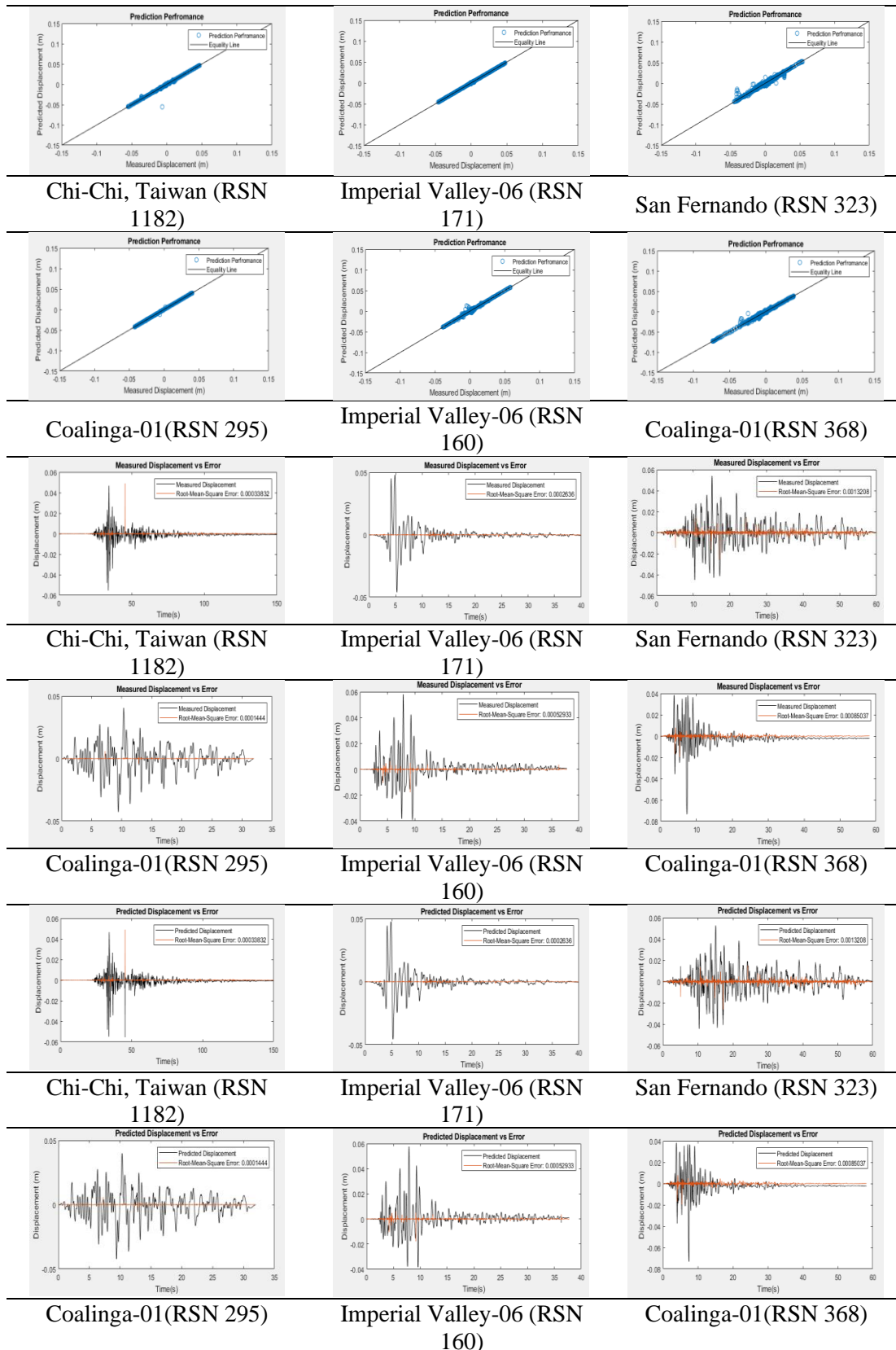
Figure 27: Validation of the proposed model for displacement in time domain for different types of earthquakes

As shown in Figure 24 and Figure 26, the proposed artificial neural system can provide high accuracy in predicting the response of the RC structure under several types of earthquake records. As can be observed from Figure 27, the maximum RMSE is 0.001 which is acceptable.

4.6 Prediction Model of the Envelope Response of Structures

In this section, five different ANN prediction configurations will be proposed. The first one will be used for estimating the peak (envelope) acceleration, the second one will be used for peak inter-story drift ratio, the third one for the peak based shear, the fourth one will be used for the peak input energy, the last one for the peak damping energy.

4.6.1 Proposed Algorithm

As mentioned previously, many engineers and scientists usually use the peak values for their design or research tasks. On such occasions, many earthquake records are used to fulfill the code requirements for the minimum number of ground motions which is considered as 11 records in ASCE 7-16. Therefore, handling such a long analysis recorders significantly long process. In this study, several ANN models are proposed each for different seismic behavior of RC structures utilizing FVDs. These models are developed in a way that they can give high accuracy in estimating the response of low-, low-to-mid, and mid-rise buildings under any type of ground motion records using a minimal number of input requirements. The developed algorithm is further compared against the conventional NTHA as shown in Figure 15.

4.6.2 Proposed ANN Configurations

As mentioned previously, five different ANN configurations were proposed in this study, as shown in Figure 28, to estimate the peak acceleration, displacement, base shear, input energy, and damping energy.

54

Roof Acceleration

PGA

PGV

PGD

PGA/PGV

Vs30

Bare Structure **Roof Acceleration** Response

C value of the FVDs

α value of the FVDs

Roof Acceleration Response of the FVD structure

Input of the Artificial Neural Network Estimation

Output of the Artificial Neural Network Estimation

Inter-Story Drift Ratio

PGA

PGV

PGD

PGA/PGV

Vs30

Bare Structure **Inter-Story Drift Ratio** Response

C value of the FVDs

α value of the FVDs

Inter-Story Drift Ratio Response of the FVD structure

Input of the Artificial Neural Network Estimation

Output of the Artificial Neural Network Estimation

Base Shear

PGA	
PGV	
PGD	
PGA/PGV	
Vs30	**Base Shear** Response of the FVD structure
Bare Structure **Base Shear** Response	
C value of the FVDs	
α value of the FVDs	
Input of the Artificial Neural Network Estimation	Output of the Artificial Neural Network Estimation

Input Energy

PGA	
PGV	
PGD	
PGA/PGV	
Vs30	**Input Energy** Response of the FVD structure
Bare Structure **Input Energy** Response	
C value of the FVDs	
α value of the FVDs	
Input of the Artificial Neural Network Estimation	Output of the Artificial Neural Network Estimation

Damping Energy

Figure 28: Proposed prediction systems for peak responses

4.6.3 Performance of the Proposed Models

In fact, for developing the general estimation model that can be accurately applied to wide range of buildings from low- to mid-rise ones, the response of a single story, three stories, and six stories RC structures utilizing various combinations of C and α values, as discussed in chapter 3, were used. The performance of the proposed models to these data that were used for developing the systems is discussed herein.
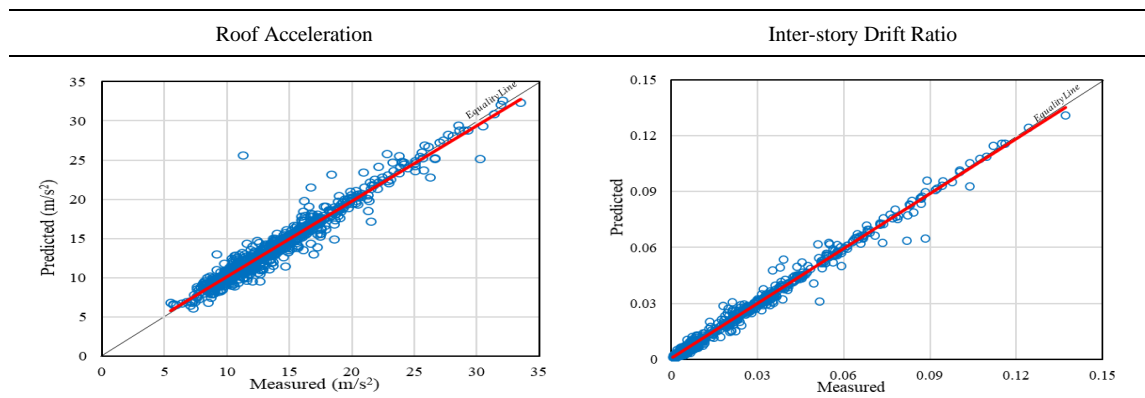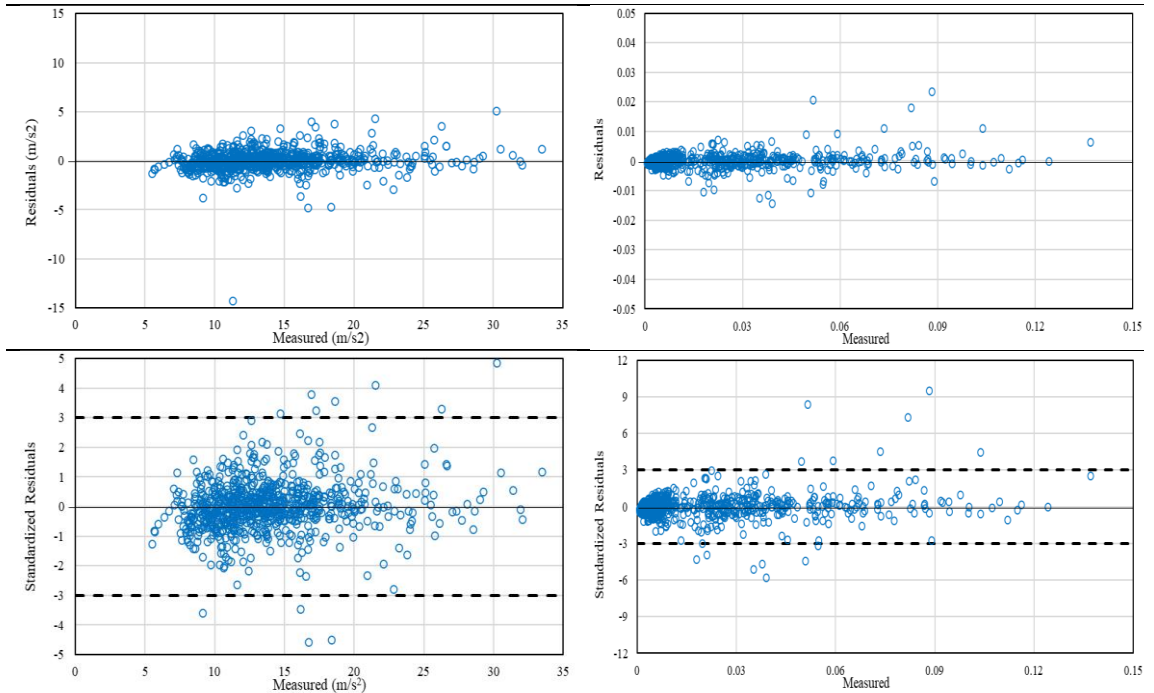
Figure 29: Performance of the proposed models for peak acceleration and inter-story
drift ratio

The roof acceleration model is shown in Figure 29. It can be seen that the proposed

setup can provide significantly high accuracy and fitting capability with an R^2 value

of 0.944. On the other hand, the model for the peak inter-story drift ratio has provided

a better performance with an R^2 value of 0.99 as shown in Figure 29. Furthermore,

based on the standardized residual analysis it can be seen that a very low number of

observations, below 1%, has exceeded the outliers limit presented in the dash lines.

Thus, it can be concluded that the proposed models give a very high capability of

fitting the data and are suitable for use in these cases.
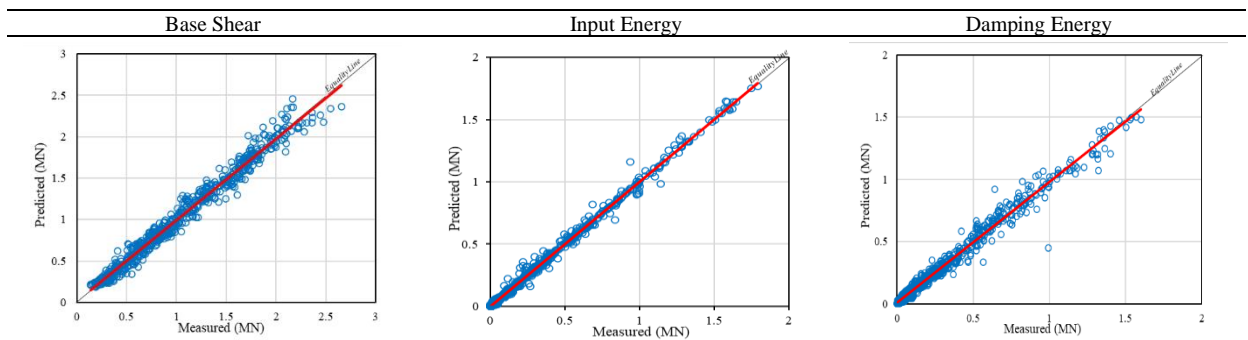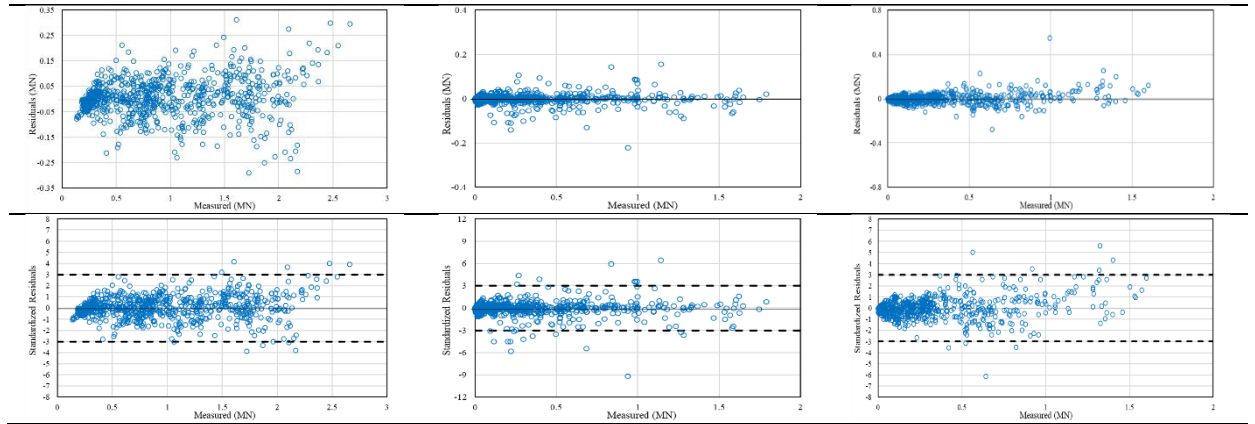
Figure 30: Performance of the proposed models for peak base shear, input energy, and damping energy

The base shear model is shown in Figure 30 holds a high accuracy and fitting capability with an R^2 value of 0.9924. Furthermore, the model for the input energy also shows very high performance with an R^2 value of 0.996 as shown in Figure 30. Moreover, the damping energy model exhibits high accuracy an R^2 0.9821 as illustrated in Figure 30. Form Figure 30, it can be clearly seen that the three models possess high accuracy, and performance and based on the standardized residual analysis it can be seen that a very low number of observations, below 1%, has exceeded the outliers limit presented in the dash lines. Thus, it can be concluded that the proposed models give a very high capability of fitting the data and are suitable for use in these cases.

4.7 Validity of the Proposed Approach for Structures with Different Number of Stories

In this section, validation of the estimation models was conducted using different levels of low-, low-to-mid-, and mid-rise buildings mainly with two, four, five stories. In addition to that, the capability of estimation models was discussed for high-rise buildings, as classified by [89] using seven, eight, and nine stories to set a limit to

which these models are suitable. The results of the validations illustrate the accurateness and effectiveness in these cases.

The validation results of roof acceleration show that the estimation model is capable of giving accurate results for low-, low-to-mid, mid-rise structures only as illustrated in Figure 31 where the accuracy drops for the roof acceleration and peak inter-story drift ratio of eight and nine stories as shown in Figure 31 where a large number of eight and nine stories observations exceeded the outliers limit.
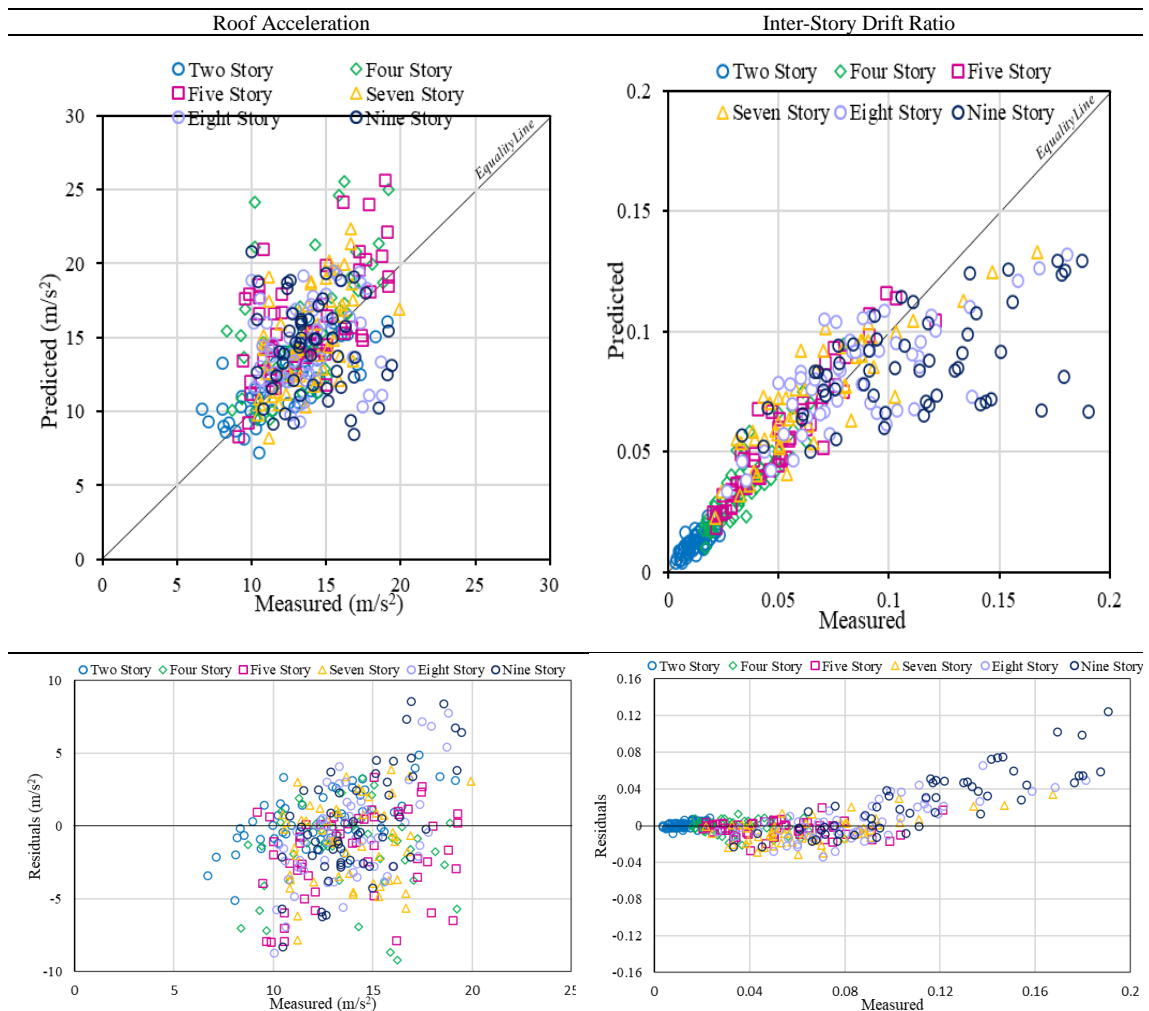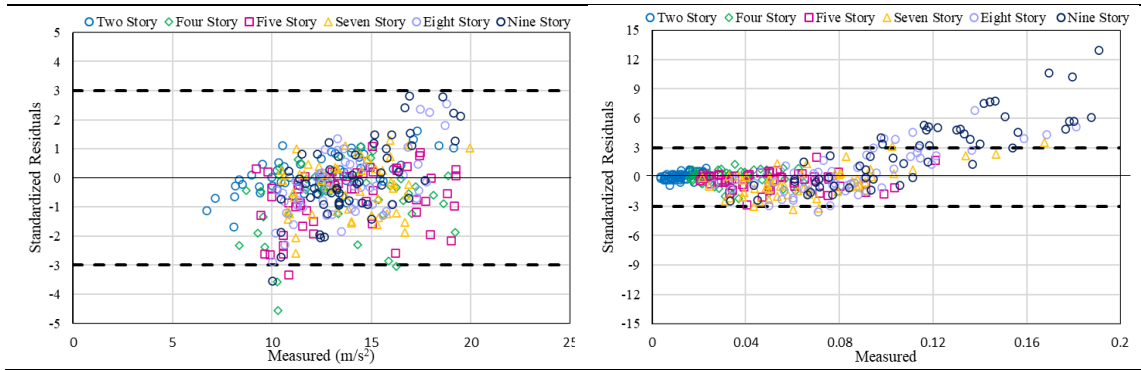
Figure 31: Validation of the proposed models for roof acceleration and peak inter-story drift ratio

The validation results of base shear, input energy, and damping energy show that the estimation models are capable of giving accurate results for low-, low-to-mid, mid-rise structures as illustrated in Figure 32 but the accuracy drops for high-rise buildings for all models of eight and nine stories as shown in Figure 32 where a large number of eight and nine stories observations exceeded the outliers limit.
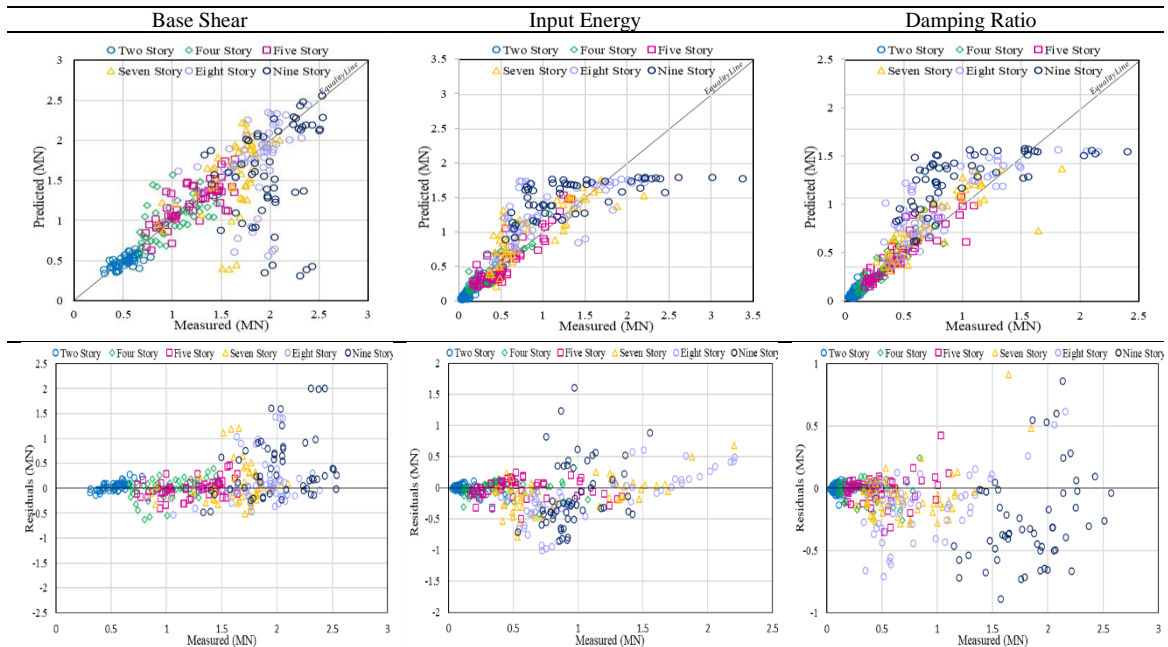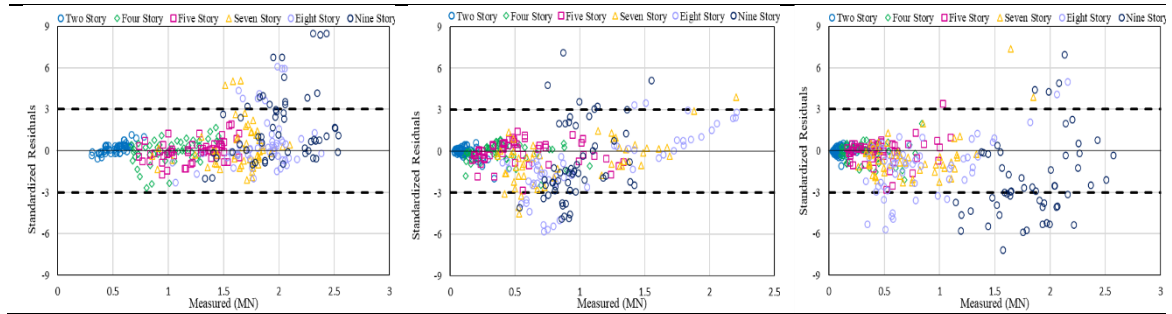
Figure 32: Validation of the proposed models for peak base shear, input energy, and damping energy

Based on the above results it can be said that the proposed modes are applicable with high accuracy up 7 stories. Whereas, 8 and 9 stories provide a low accuracy which means that they can be used safely to the maximum cases of mid-rise buildings. Such a conclusion is mainly driven due to the fact that the prediction models were intended for low-, low-to-mid, and mid-rise buildings that can be considered as the most common cases of RC moment-resisting framed structures constructed in the Middle East area.

Chapter 5

CONCLUSIONS

This thesis has focused on ANN approaches to establish different prediction models capable of accurately estimating the responses of low, low-to-mid, and mid-rise RC 2D structures equipped with FVDs in the time domain and as peak (envelope) without the need of performing analysis for structures with FVDs. An extensive number of nonlinear time history analyses on different types of RC structures utilized with FVDs under different characteristics of ground motion inputs in order to indicate the most significant parameters needed to be taken into account for establishing the mathematical estimation models was performed. The results indicate that the prediction models of the responses in the time domain and as peak (envelope) hold very high accuracy and superior performance in comparison to conventional NTHA in terms of time, effort, and cost. However, the estimation model was established for multiple simple cases of FVDs arrangement in the structure where dampers are placed as a zig-zag shape in the mid-span and hence, other arrangements of FVDs were not considered during the establishment of the input dataset since the aim of the thesis was to assess and investigate the applicability of predicting the responses in the time domain and as peak (envelope) of RC structures utilized with FVDs via ANN. On the other hand, the estimation model was intended to be applicable for predicting the responses of RC low, low-to-mid, and mid-rise buildings to represent the common wide range structures in the Middle East region. Future investigations can be done to provide a new prediction model for the cases of high-rise buildings that might range

from 9 to over 25 stories of RC moment-resisting frames utilizing FVDs. The results of the thesis will open the door for a new approach of analysis and design of structures by estimating the responses of the RC structure equipped with FVDs without the need of performing NTHA on them by means of implementing the knowledge of ANN which can significantly decrease the effort, time and cost in which the proposed estimation models need one-fourth of the time to build the model and determine the results in comparison to NTHA which results in faster, minimized cost and effort approach. In addition to that, the proposed prediction models exhibited high performance and accurateness in estimating the responses of RC structures.

5.1 Future Works

Further research is still needed in the field of fluid viscous dampers to provide a solid prediction model that works for high rise and tall structures. In addition to that, future works need to focus on proposing an optimized design method that takes into account the characteristics of the earthquakes being used and the capabilities and properties of the fluid viscous dampers being utilized.

REFERENCES

[1] Moustafa, Gheni and ElGawady, "Shaking-table testing of high energy–dissipating rubberized concrete columns," *Journal of Bridge Engineering,* vol. 22, no. 8, p. 04017042, 2017.

[2] Habib, Yildirim and Eren, "Column repair and strengthening using RC jacketing: a brief state-of-the-art review," *Innovative Infrastructure Solutions,* vol. 5, no. 3, pp. 1-11, 2020.

[3] Lu, Wang, Zhou and Lu, "Nonlinear dissipative devices in structural vibration control: A review," *Journal of Sound and Vibration,* vol. 423, pp. 18-49, 2018.

[4] D. Domenico, Ricciardi and Takewaki, "Design strategies of viscous dampers for seismic protection of building structures: a review," *Soil Dynamics and Earthquake Engineering,* vol. 118, pp. 144-165, 2019.

[5] Taylor, "Smart buildings and viscous dampers—a design engineer's perspective," *The Structural Design of Tall and Special Buildings,* vol. 19, no. 4, pp. 369-372, 2010.

[6] Harris and Piersol, Harris' shock and vibration handbook, vol. 5, New York: McGraw-Hill, 2002.

[7] Douglas, "History, design, and applications of fluid dampers in structural engineering," in *In Proceedings of structural engineers world congress*, Japan, 2002.

[8] Symans, Charney, Whittaker, Constantinou, Kircher, Johnson and McNamara, "Energy dissipation systems for seismic applications: current practice and recent developments," *Journal of structural engineering,* vol. 134, no. 1, pp. 3-21, 2008.

[9] Hwang, Tsai, Wang and Huang, "Experimental study of RC building structures with supplemental viscous dampers and lightly reinforced walls," *Engineering structures,* vol. 28, no. 3, pp. 1816-1824, 2006.

[10] Taylor and Constantinou, "Testing procedures for high output fluid viscous dampers used in building and bridge structures to dissipate seismic energy.," *Shock and Vibration,* vol. 2, no. 5, pp. 373-381, 1995.

[11] Constantinou and Symans, "Experimental study of seismic response of buildings with supplemental fluid dampers," *The Structural Design of Tall Buildings,* vol. 2, no. 2, pp. 93-132, 1993.

[12] Lee and Taylor, "Viscous damper development and future trends," *The Structural Design of Tall Buildings,* vol. 10, no. 5, pp. 311-320, 2001.

[13] Lin, Liu and Tsai, "Real-valued modal response history analysis for asymmetric-plan buildings with nonlinear viscous dampers," *Soil Dynamics and Earthquake Engineering,* vol. 77, pp. 97-110, 2015.

[14] Lu, Wang, Zhou and Lu, "Nonlinear dissipative devices in structural vibration control: A review," *Journal of Sound and Vibration,* vol. 423, pp. 18-49, 2018.

[15] D. Paola and Navarra, "Stochastic seismic analysis of MDOF structures with nonlinear viscous dampers," *Structural Control and Health Monitoring: The Official Journal of the International Association for Structural Control and Monitoring and of the European Association for the Control of Structures,* vol. 16, no. 3, pp. 303-318, 2009.

[16] Soong and Costantinou, Passive and active structural vibration control in civil engineering, vol. 345, Springer, 1994.

[17] Lee, Min, Hwang and Kim, "Evaluation of equivalent damping ratio of a structure with added dampers," *Engineering Structures,* vol. 26, no. 3, pp. 335-346, 2004.

[18] Narkhede and Sinha, "Behavior of nonlinear fluid viscous dampers for control of shock vibrations," *Journal of Sound and Vibration,* vol. 333, no. 1, pp. 80-98, 2014.

[19] Lin and Chopra, "Earthquake response of elastic SDF systems with non-linear fluid viscous dampers," *Earthquake engineering & structural dynamics,* vol. 31, no. 9, pp. 1623-1642, 2002.

[20] Paola, Mendola and Navarra, "Stochastic seismic analysis of structures with nonlinear viscous dampers," *Journal of Structural Engineering,* vol. 133, no. 10, pp. 1475-1478, 2007.

[21] Wen, "Methods of random vibration for inelastic structures," *Applied Mechanics Reviews,* vol. 42, no. 2, pp. 39-52, 1989.

[22] Roberts and Spanos, Random vibration and statistical linearization, New York: Dover Publications, 2003.

[23] Grossmayer and Iwan, "A linearization scheme for hysteretic systems subjected to random excitation," *Earthquake Engineering & Structural Dynamics,* vol. 9, no. 2, pp. 171-185, 1981.

[24] Takewaki, "Probabilistic critical excitation for MDOF elastic–plastic structures on compliant ground," *Earthquake engineering & structural dynamics,* vol. 30, no. 9, pp. 1345-1360, 2001.

[25] Wong, "Seismic energy analysis of structures with nonlinear fluid viscous dampers—algorithm and numerical verification," *The Structural Design of Tall and Special Buildings,* vol. 20, no. 4, pp. 482-496, 2011.

[26] Landi, Fabbri and Diotallevi, "A two-step direct method for estimating the seismic response of nonlinear structures equipped with nonlinear viscous dampers," *Earthquake engineering & structural dynamics,* vol. 43, no. 11, pp. 1641-1659, 2014.

[27] Tubaldi, Ragni and Dall'Asta, "Probabilistic seismic response assessment of linear systems equipped with nonlinear viscous dampers," *Earthquake Engineering & Structural Dynamics,* vol. 44, no. 1, pp. 101-120, 2015.

[28] Kougioumtzoglou and Spanos, "An approximate approach for nonlinear system response determination under evolutionary stochastic excitation," *urrent science,* pp. 1203-1211, 2009.

[29] T. Dall′ Asta and Ragni, "Influence of the nonlinear behavior of viscous dampers on the seismic demand hazard of building frames," *Earthquake Engineering & Structural Dynamics,* vol. 45, no. 1, pp. 149-169, 2016.

[30] K. L. Fujita and Takewaki, "Optimal placement and design of nonlinear dampers for building structures in the frequency domain," *Earthquakes and Structures,* vol. 7, no. 6, pp. 1025-1044, 2014.

[31] Martinez-Rodrigo and Romero, "An optimum retrofit strategy for moment resisting frames with nonlinear viscous dampers for seismic applications," *Engineering Structures,* vol. 25, no. 7, pp. 913-925, 2003.

[32] Su, Huang and Ma, "Fast equivalent linearization method for nonlinear structures under nonstationary random excitations," *Journal of Engineering Mechanics,* vol. 142, no. 8, p. 04016049, 2016.

[33] Lin, Chang and Chen, "Direct displacement-based design for seismic retrofit of existing buildings using nonlinear viscous dampers," *Bulletin of Earthquake Engineering,* vol. 6, no. 3, pp. 535-552, 2008.

[34] Pekcan, Mander and Chen, "Fundamental considerations for the design of non-linear viscous dampers," *Earthquake engineering & structural dynamics,* vol. 28, no. 11, pp. 1405-1425, 1999.

[35] Arima, Miyazaki, Tanaka and Yamazaki, "A study on buildings with large damping using viscous damping walls," *In Proceedings of the 9th world conference on earthquake engineering,* vol. 821, 1988.

[36] Yeung and Pan, "The effectiveness of viscous-damping walls for controlling wind vibrations in multi-story buildings," *Journal of Wind Engineering and Industrial Aerodynamics,* vol. 77, pp. 337-348, 1998.

[37] Lu, Zhou and Yan, "Shaking table test and numerical analysis of RC frames with viscous wall dampers," *Journal of structural engineering,* vol. 134, no. 1, pp. 64-76, 2008.

[38] Soong and Spencer, "Supplemental energy dissipation: state-of-the-art and state-of-the-practice," *Engineering structures,* vol. 24, no. 3, pp. 243-259, 2002.

[39] Makris, Constantinou and Dargush, "Analytical model of viscoelastic fluid dampers," *Journal of Structural Engineering,* vol. 119, no. 11, pp. 3310-3325, 1993.

[40] Lin and Chopra, "Asymmetric one-storey elastic systems with non-linear viscous and viscoelastic dampers: Simplified analysis and supplemental damping system design," *Earthquake engineering & structural dynamics,* vol. 32, no. 4, pp. 579-596, 2003.

[41] Ras and Boumechra, "Study of nonlinear fluid viscous dampers behaviour in seismic steel structures design," *Arabian Journal for Science and Engineering,* vol. 39, no. 12, pp. 8635-8648, 2014.

[42] Main and Jones, "Free vibrations of taut cable with attached damper. II: Nonlinear damper," *Journal of engineering mechanics,* vol. 128, no. 10, pp. 1072-1081, 2002.

[43] Chung, Wu, Huang, Chang and Lien, "Optimal design theories of tuned mass dampers with nonlinear viscous damping," *Earthquake engineering and engineering vibration,* vol. 8, no. 4, pp. 547-560, 2009.

[44] Taylor and Duflot, "Fluid viscous dampers used for seismic energy dissipation in structures," in *In Proceedings of the 12th European Conference on Earthquake Engineering*, 2002.

[45] Setyawati, Sahirman and Creese, "Neural networks for cost estimation," *AACE International Transactions,* 2002.

[46] Elha and Boussabaine, "An artificial neural system for cost estimation of construction projects," in *In Proceedings of the 14th ARCOM annual conference*, Liverpool, 1998.

[47] Agatonovic-Kustrin and Beresford, "Basic concepts of artificial neural network (ANN) modeling and its application in pharmaceutical research," *Journal of pharmaceutical and biomedical analysis,* vol. 22, no. 5, pp. 717-727, 2000.

[48] M. Y. Rafiq, G. Bugmann and D. J. Easterbrook, "Neural network design for engineering applications," *Computers & Structures,* vol. 79, no. 17, pp. 1541-1552, 2001.

[49] R. Hecht-Nielsen, Neurocomputing, Addison-Wesley, 1990.

[50] Azar, "Fast neural network learning algorithms for medical applications," *Neural Computing and Applications,* vol. 23, no. 3-4, pp. 1019-1034, 2013.

[51] Fletcher, Practical methods of optimization, John Wiley & Sons, 2013.

[52] Curtis and Que, "A quasi-Newton algorithm for nonconvex, nonsmooth optimization with global convergence guarantees," *Mathematical Programming Computation,* vol. 7, no. 4, pp. 399-428, 2015.

[53] Burden and Winkler, "Bayesian regularization of neural networks. In Artificial neural networks," in *Artificial Neural Networks Methods and Applications* , Humana Press, 2008, pp. 23-42.

[54] Sorich, Miners, McKinnon, Winkler, Burden and Smith, "Comparison of linear and nonlinear classification algorithms for the prediction of drug and chemical metabolism by human UDP-glucuronosyltransferase isoforms," *Journal of chemical information and computer sciences,* vol. 43, no. 6, pp. 2019-2024, 2003.

[55] Xu, Zeng, Xu, Huang, Jiang and Sun, "Application of Bayesian regularized BP neural network model for trend analysis, acidity and chemical composition of precipitation in North Carolina," *Water, Air, and Soil Pollution,* vol. 172, no. 1-4, pp. 167-184, 2006.

[56] Saini and Soni, "Artificial neural network-based peak load forecasting using conjugate gradient methods," *IEEE Transactions on Power Systems,* vol. 17, no. 3, pp. 907-912, 2002.

[57] Chatterjee, "A fletcher–reeves conjugate gradient neural-network-based localization algorithm for wireless sensor networks," *IEEE transactions on vehicular technology,* vol. 59, no. 2, pp. 823-830, 2009.

[58] Bishop, Pattern recognition and machine learning, springer, 2006.

[59] Dreyfus, Neural networks: methodology and applications, Springer Science & Business Media, 2005.

[60] Du and Stephanus, "Levenberg-Marquardt neural network algorithm for degree of arteriovenous fistula stenosis classification using a dual optical photoplethysmography sensor," *Sensors,* vol. 18, no. 7, p. 2322, 2018.

[61] Marquardt, "An algorithm for least-squares estimation of nonlinear parameters," *Journal of the society for Industrial and Applied Mathematics,* vol. 11, no. 2, pp. 431-441, 1963.

[62] Hagan and Menhaj, "Training feedforward networks with the Marquardt algorithm," *IEEE transactions on Neural Networks,* vol. 5, no. 6, pp. 989-993, 1994.

[63] Cömert and Kocamaz, "A study of artificial neural network training algorithms for classification of cardiotocography signals," *J Sci Technol,* vol. 7, no. 2, pp. 93-103, 2017.

[64] Lv, Xing, Zhang, Na, Li, Liu, ... and Wang, "Levenberg–Marquardt backpropagation training of multilayer neural networks for state estimation of a safety-critical cyber-physical system," *IEEE Transactions on Industrial Informatics,* vol. 14, no. 8, pp. 3436-3446, 2017.

[65] Ahmed, Ali, Elkatatny and Abdulraheem, "New Artificial Neural Networks Model for Predicting Rate of Penetration in Deep Shale Formation," *Sustainability,* vol. 11, no. 22, p. 6527, 2019.

[66] NIST, "Guidelines for Nonlinear Structural Analysis for Design of Buildings Part IIb – Reinforced Concrete Moment Frames," National Institute of Standards and Technology, 2017.

[67] J. B. Mander, M. J. Priestley and R. Park, "Theoretical stress-strain model for confined concrete," *Journal of structural engineering,* vol. 114, no. 8, pp. 1804-1826, 1988.

[68] R. Park and T. Paulay, Reinforced Concrete Structures, Wiley , 1975.

[69] Avşar, Bayhan and Yakut, "Effective flexural rigidities for ordinary reinforced concrete columns and beams," *The Structural Design of Tall and Special Buildings,* vol. 23, no. 6, pp. 463-482, 2014.

[70] Kwon, Strength, Stiffness, and Damage of Reinforced Concrete Buildings, Austin, Texas: University of Texas at Austin, 2016.

[71] Kalantari and Roohbakhsh, "Expected seismic fragility of code-conforming RC moment resisting frames under twin seismic events," *Journal of Building Engineering,* vol. 28, p. 101098, 2020.

[72] Baker, "Quantitative classification of near-fault ground motions using wavelet analysis," *Bulletin of the Seismological Society of America,* vol. 97, no. 5, pp. 1486-1501, 2007.

[73] Hu, Wang, Huang, Li and Luo, "Seismic mitigation performance of structures with viscous dampers under near-fault pulse-type earthquakes," *Engineering Structures,* vol. 23, p. 109878, 2020.

[74] A. T. Council, Quantification of building seismic performance factors, California: US Department of Homeland Security, FEMA, 2009.

[75] ASCE, ASCE/SEI 7-05: Minimum design loads for buildings and other structures, Virginia: American Society of Civil Engineers, 2005.

[76] P. E. E. R. (. Center, "Technical report for the PEER ground motion database web application," Pacific Earthquake Engineering Research (PEER) Center, 2010.

[77] D. Michaud and P. Léger, "Ground motions selection and scaling for nonlinear dynamic analysis of structures located in Eastern North America," *Canadian journal of civil engineering,* vol. 41, no. 3, pp. 232-244, 2013.

[78] S. Kitayama and M. C. Constantinou, "Seismic Performance of Buildings with Viscous Damping Systems Designed by the Procedures of ASCE/SEI 7-16," *Journal of Structural Engineering,* vol. 144, no. 6, p. 04018050, 2018.

[79] Xi, "Performance based implementation of seismic protective devices for structures," Doctoral dissertation, UCLA, Los Angeles, 2014.

[80] Hwang, "Viscous dampers: practical application issues for the structural engineer," Doctoral dissertation, Massachusetts Institute of Technology, MASSACHUSETTS, 1998.

[81] Adam and Smith, "Active tensegrity: A control framework for an adaptive civil-engineering structure," *Computers & Structures,* vol. 86, no. 23-24, pp. 2215-2223, 2008.

[82] Prasad, Eskandari and Reddy, "Prediction of compressive strength of SCC and HPC with high volume fly ash using ANN," *Construction and Building Materials,* vol. 23, no. 1, pp. 117-128, 2009.

[83] Lee, Lin and Lu, "Assessment of highway slope failure using neural networks," *Journal of Zhejiang University-SCIENCE A,* vol. 10, no. 1, pp. 101-108, 2009.

[84] Das, Samui and Sabat, "Application of artificial intelligence to maximum dry density and unconfined compressive strength of cement stabilized soil," *Geotechnical and Geological Engineering,* vol. 29, no. 3, pp. 329-342, 2011.

[85] Okoh, Computer neural networks on MATLAB, North Charleston: CreateSpace Independent Publishing Platform, 2016.

[86] Wei, Zhuo, Li and Yang, "Parameter optimization of a vertical spring-viscous damper-Coulomb friction system," *Shock and Vibration,* vol. 2019, 2019.

[87] Goel, "Seismic response study of asymmetric systems with linear and nonlinear fluid viscous dampers," Civil and Environmental Engineering, 2002.

[88] Impollonia and Palmeri, "Seismic performance of buildings retrofitted with nonlinear viscous dampers and adjacent reaction towers," *Earthquake Engineering & Structural Dynamics,* vol. 47, no. 5, pp. 1329-1351, 2018.

[89] Elnashai and D. Sarno, Fundamentals of earthquake engineering, Wiley, 2015.

APPENDICES

Appendix A: MATLAB Code for Artificial Neural Network

```matlab
clear all; fclose all; clc;
if isdir('networks')==0
    mkdir('networks');
end

%Import data
inputs=dlmread('inputs.txt', '\t', 1, 0);    %input data
targets=dlmread('outputs.txt', '\t', 1, 0);  %target data
inputs = inputs';   %transpose the data
targets = targets'; %transpose the data
net = newff(inputs,targets,[50 50 50 50 50]); % traing the algorithm for 5 hidden layers using 50 neurons in each
net.trainParam.epochs = 10000;
net = train(net,inputs,targets);
Y = sim(net,inputs);
```

Appendix B: MATLAB Code for Artificial Neural Network

```matlab
>> Fitting = (1 - sum((m - p).^2)/sum((m - mean(m)).^2))*100; % Coefficient of Determination to  represent goodness of fitting
E = round( Fitting , 2 );
RMSE = sqrt( sum( (m(:)-p(:)).^2) / numel(m) ); % Root mean square error
subplot(2,2,1);
plot(t,m) % Comparing Measured Response vs Predicted Response
hold on
plot(t,p)
title('Measured Response vs Predicted Response')
legend('Measured Response',['Predicted Response: %' num2str(E)]);
xlabel('Time(s)')
ylabel('Response')
subplot(2,2,2);
plot(t,m)% Measured Response vs Error
hold on
plot(t,Residuals)
title('Measured Response vs Error')
legend('Measured Response',['Root-Mean-Square Error: ' num2str(RMSE)]);
xlabel('Time(s)')
ylabel('Response')
subplot(2,2,3);
plot(t,p)% Predicted Response vs Error
hold on
plot(t,Residuals)
title('Predicted Response vs Error')
legend('Predicted Response',['Root-Mean-Square Error: ' num2str(RMSE)]);
xlabel('Time(s)')
ylabel('Response')
subplot(2,2,4);
scatter(m,p)% Measured Response vs Predicted Response
hold on
plot([-20 20],[-20 20])
title('Prediction Perfromance')
legend('Prediction Perfromance',['Equality Line']);
xlabel('Measured Response')
ylabel('Predicted Response')
```